C01

Immunogold labelling for glutamate in lanceolate endings of rat hairs

F.C. Shenton[1], H. Wollner[1], G.S. Bewick[2] and R.W. Banks[1]

[1]School of Biological & Biomedical Sciences, Durham University, Durham, UK and [2]School of Medical Sciences, Aberdeen University, Aberdeen, UK

50 nm diameter, clear synaptic-like vesicles (SLVs) are found in primary mechanosensory nerve terminals. Our studies of sensory endings of rat Ia afferents suggest SLVs are part of a glutamatergic system that modulates mechanoreceptor excitability; in particular, glutamate-like immunoreactivity indicated a high glutamate content in these endings (Bewick et al, 2005). We now show that lanceolate endings of rat hair follicles also have high levels of glutamate. Adult rats (3) were deeply anaesthetized with sodium pentobarbitone (45 mg kg–1, I.P.) and fixed by transcardial perfusion (2% paraformaldehyde and 2.5% glutaraldehyde in 0.1M phosphate buffer, pH 7.4). Samples of pinna skin and cerebellum (positive control) were embedded in Araldite for post-embedding immunocytochemistry using rabbit polyclonal antibodies (Sigma) against glutamate or GABA. 10nm gold-labelled antibody (goat anti-rabbit IgG, BBInternational) was used for secondary incubation. EMgraphs (magnification 40000 to 60000x) were analysed with ImageJ (NIH, USA). Profiles of lanceolate endings and their accessory cells of skin; and mossy fibres, granule cells and Golgi cells of cerebellum were sampled for quantification. Glutamate-specific labelling was greater in lanceolate endings (mean 28.2 ± SE 1.73 gold particles/μm2, n = 84) than in the surrounding accessory cells (mean 9.3 ± SE 0.80 particles/μm2, n = 84; P ≤ 0.002, ANOVA and post hoc Tukey test), and was similar to that in mossy fibres (mean 28.2 ± SE 2.39 particles/μm2, n = 28) and granule cells (mean 22.6 ± SE 1.13 gold particles/μm2, n = 45). GABA-specific immunoreactivity was not found in either the lanceolate endings or accessory cells of the skin. However anti-GABA immunoreactivity was evident in the cerebellum, particularly in Golgi-cell axons.

In conclusion these data support our hypothesis that regulation of mechanoreceptor function by glutamate release from SLVs may be a general modulatory mechanism, common to other mechanosensitive structures in addition to muscle spindles.

Bewick, G. S., B. Reid, et al. (2005). "Autogenic modulation of mechanoreceptor excitability by glutamate release from synaptic-like vesicles: evidence from the rat muscle spindle primary sensory ending." Journal of Physiology-London 562(2): 381-394.

Where applicable, the authors confirm that the experiments described here conform with The Physiological Society ethical requirements.

C02

Glutamatergic modulation of vesicle turnover in primary mechanosensory endings

P. Singh[1], A. Simon[1], R.W. Banks[2] and G.S. Bewick[1]

[1]School of Medical Sciences, University of Aberdeen, Aberdeen, UK and [2]School of Biological and Biomedical Sciences, University of Durham, Durham, UK

Primary mechanosensory nerve terminals in vertebrates contain clear synaptic-like vesicles (SLVs). Previously autogenic modulation of mechanoreceptor excitability by glutamate release from SLVs has been demonstrated (Bewick et al, 2005) using Ia afferent primary endings of rat muscle spindle as a model. Our aim here was to test whether SLVs in other endings are functionally similar, using mechanosensitive lanceolate endings of mouse hair follicles. FM1-43 was used to characterise SLV recycling in lanceolate endings. C57/B16J mice (20 - 28 g, either sex) were killed by Schedule 1 methods, ASPA (1986). The inner and outer layers of ear skin were separated, cleaned and equilibrated in carboxygenated physiological solution (1 hr, 30°C). After labelling (30 min, 10 μM) in saline or test solution, FM1-43 was washed off (30 min) and then chelated (1 mM ADVASEP-7, 5 min). Fluorescent microscope images were saved on computer hard drive. Differences in net fluorescence intensity were compared (3-4 ears per group) for control (n = 33-40 terminals) and treated preparations by Student's *t*-test, with a significance threshold of $P < 0.05$. Consistent with previous studies (Kain & Slater, 2003) 1 mM neomycin and 10 mM Ca^{2+} did not block FM1-43 uptake (n = 32; $P = 0.117$). Labelling was reversible, as terminals destained spontaneously. The dye release mechanism was tested with 3 nM α-latrotoxin, which elicits uncontrolled exocytosis. Latrotoxin markedly increased loss (52% at 15 min, n = 7, $P < 0.0001$; 70% at 30 min, n = 7, $P < 0.0001$) of label from terminals, indicating dye loss was predominantly through exocytosis. These data suggest dye fluxes were through SLV recycling, not mechanically sensitive channels. However, 3 mM Co^{2+} and 5 mM Mg^{2+} blocked FM1-43 labelling by 91.3% (n = 43; $P < 0.001$) and 71.5% (n = 39; $P < 0.001$), suggesting SLV recycling is Ca sensitive. Labelling was sensitive to glutamate since 1 mM doubled net terminal intensity (n = 34; $P < 0.001$). Conversely, 10 μM PCCG-13, a specific blocker of the non-canonical phospholipase D mGlu receptor, decreased dye uptake by 75% (n = 34; $P < 0.001$). 100 nM 5-fluoro-2-indolyldes-chlorohalopemide (FIPI) a new, highly specific PLD inhibitor (Monovich *et al.*, 2007) also reduced net intensity by > 33% (n = 42; $P < 0.01$). These data suggest SLV recycling in lanceolate nerve endings and muscle spindle afferents share similar functional characteristics, and is sensitive to glutamate. This is consistent with a general role for SLVs in glutamatergic modulation of mechanosensation.

Bewick GS, Reid B, Richardson C & Banks RW (2005). *J Physiol* **562**, 381-394.

Kain N & Slater CR (2003). *BNA Abstr* **17**, P101.

Monovich L, *et al.*, (2007). *Bioorg Med Chem Lett* **17**, 2310-2311.

This work was supported by the MRC. FIPI was a generous gift from Novartis Inc. alpha-Latrotoxin was a generous gift from Prof. Yuri Ushkaryov, Imperial College, London.

Where applicable, the authors confirm that the experiments described here conform with The Physiological Society ethical requirements.

C03

Defective functional maturation of inner hair cells in myosin VIIa mutant mice

K.M. Ranatunga and C.J. Kros

School of Life Sciences, University of Sussex, Brighton, UK

Mutations in the *Myo7a* gene that encodes the unconventional, non-muscle myosin, Myosin VIIa, are associated with Usher syndrome Ib, a rare genetic disorder that leads to deaf-blindness in humans, as well as non-syndromic deafness (1). In *Shaker-1* mice, the orthologous recessive gene also causes deafness with impaired cochlear function and progressively disorganized stereocilia of the auditory hair cells (1). Mechano-electrical transduction in hair cells of mutants deficient in Myosin VIIa is impaired requiring force on the bundle beyond the physiological range (2).

Inner hair cell basolateral currents and voltage responses were recorded from acutely dissected organ of Corti preparations of homozygous mutant and heterozygous control *Myo7a^{6J}* mutant mice using the whole-cell patch-clamp technique as previously described (3). These mice carry a missense mutation of arginine to proline in the motor domain of Myosin VIIa, resulting in an 80% reduction in expression levels of Myosin VIIa that is presumed dysfunctional (4). All data are presented as Mean±SEM (number of cells). Statistical significance was evaluated with the unpaired t-test.

We demonstrate, for the first time, that adult *Myo7a^{6J}/Myo7a^{6J}* (P20-P30) inner hair cells retain immature electrical properties (3). The fast, outward potassium current $I_{K,f}$, normally expressed by around P12, is absent: measured at -25 mV it was -340±37 pA (n=6) in *Myo7a^{6J}/Myo7a^{6J}* (Fig 1A) and 1330±390 pA (n=5) in *+/Myo7a^{6J}* controls (Fig 1B); $p<0.01$. The cells display immature-like stimulated spiking behaviour (n=8) (Fig 1C) unlike the typically mature graded receptor potentials of age-matched *+/Myo7a^{6J}* controls (n=4) (Fig 1D).

Neonatal (P2-P4) *Myo7a^{6J}/Myo7a^{6J}* mutants (n=10) show spontaneous and evoked spiking behaviour like *+/Myo7a^{6J}* controls (n=8). Also the outward potassium currents of neonatal (P2-P4) *Myo7a^{6J}/Myo7a^{6J}* and *+/Myo7a^{6J}* hair cells are similar: 2470±290 pA (n=9) and 2470±370 pA (n=8) respectively measured at –25 mV; $p>0.05$.

These data explicitly show that lack of Myosin VIIa not only impairs mechano-electrical transduction but also causes dysfunctional development of inner hair cell basolateral currents.

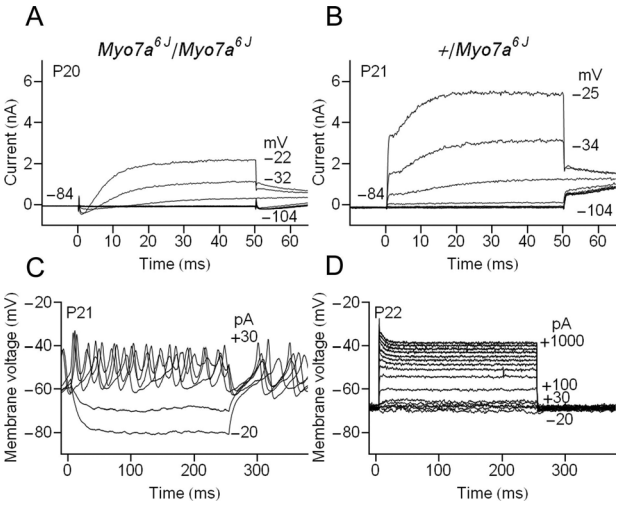

Figure 1 Inner hair cells from *Myo7a^{6J}/Myo7a^{6J}* adult mice retain immature electrophysiological properties. Basolateral currents were elicited by 50 ms voltage-steps from –120 mV to +50 mV in 10 mV increments followed by a step to -40 mV. Selected current traces from representative cells are presented for a *Myo7a^{6J}/Myo7a^{6J}* mutant (A) and a *+/Myo7a^{6J}* control (B). Voltage responses were measured in response to 250 ms current injection steps from –20 pA to +50 pA in 10 pA increments and, in addition, –200 pA to 1000 pA in 100 pA increments for *+/Myo7a^{6J}* control. Selected voltage traces are presented for a *Myo7a^{6J}/Myo7a^{6J}* mutant (C) and a *+/Myo7a^{6J}* control (D). Levels of voltage-step/current injection and age of animal are as indicated. All experiments were performed at ~34-36°C.

Petit C *et al.* (2001) *Annual Review of Genetics* **35**, 589-645.

Kros *et al.* (2002) *Nature Neuroscience* **5**, 41 – 47.

Kros *et al.* (1998) *Nature* **394**, 281-284.

Hasson *et al.* (1997) *Cell Motility and the Cytoskeleton* **37**, 127-138.

Supported by the Medical Research Council and EuroHear.

Where applicable, the authors confirm that the experiments described here conform with The Physiological Society ethical requirements.

C04

Transducer-transporter coupling in the cochlear sensory cells

P. Mistrik[1,2], N. Daudet[1] and J. Ashmore[1,2]

[1]Ear Institute, UCL, London, UK and [2]Department of Neuroscience, Physiology and Pharmacology, UCL, London, UK

Prestin (SLC26A5) is a molecular actuator found in mammalian cochlear outer hair cells (OHCs) and implicated in the amplification of sound in the inner ear. One of the issues has been that OHCs need to serve as a universal power source over a broad frequency range, and it has often been claimed that the receptor potentials will be so attenuated by the membrane electrical filtering that other mechanisms need to be invoked at high acoustic frequencies. To address this point we have used a large-scale computational model of cochlear current flow to analyse the transmembrane potentials in OHCs when the cells are embedded in the intact cochlea (Mistrik P *et al.*, 2009). This *in silico* model has allowed us to conclude that the known gradient in OHC conductance between cochlear base and apex effectively counteracts the single-cell membrane capacitance at high

frequencies. The calculated attenuation of the OHC receptor potential was 6 dB/decade (instead of 21 dB/decade) in the presence (or absence, respectively) of the gradient. This low attenuation suggests that forces generated by OHCs can indeed provide power input over the whole auditory frequency range. A further consideration of the contribution of prestin to cochlear function was guided by the analysis of its amino acid sequence. Prestin belongs to a family SLC26 of solute carriers, members of which exchange halides for SO_4^{2-} or HCO_3^-. To determine if prestin is also a bicarbonate transporter, we linked prestin to super-ecliptic pHluorin to provide a sensitive fluorescence probe of intracellular pH (pH_{in}) near the plasma membrane. Prestin was expressed heterologously in CHO cells. Measuring the initial rate of the pH_{in} recovery from the CO_2-induced acidification showed that pH_{in} recovered 4 times faster in cells transfected with prestin, but only in the presence of extracellular HCO_3^-. Such acceleration required extracellular Cl^- to be lowered to 2 mM to establish a gradient to drive HCO_3^- into the cell. Such a mechanism was simulated by a computational model of CO_2- HCO_3^- exchange. The transport process was significantly reduced by extracellular application of 10 mM salicylate, an agent which inhibits OHC forces. These data therefore suggest that prestin does act as a weak HCO_3^-/ Cl^- antiporter, effects anticipated to be much greater in OHCs than in CHO cells as a result of the 30x higher copy number for prestin. The proposal suggests that intracellular chloride in OHCs may be under metabolic control.

These results indicate that, in addition to participating in wide band cochlear sound amplification, prestin may also be involved in many slower time scale (>10s) cochlear phenomena where changes in OHC stiffness and turgor pressure have been implicated.

Mistrík P *et al.* (2009) J R Soc Interface. **6**,279-91.

This research was supported by European Commission FP6 Integrated Project EUROHEAR, LSHG-CT-20054-512063.

Where applicable, the authors confirm that the experiments described here conform with The Physiological Society ethical requirements.

C05

The development of glycinergic inhibition in the spinal dorsal horn

S. Koch[1], G. Hathway[2,1] and M. Fitzgerald[1]

[1]Department of Neuroscience, Physiology and Pharmacology, UCL, London, UK and [2]School of Biomedical Sciences, University of Nottingham, Nottingham, UK

Newborn spinal sensory circuits are poorly organised: reflex thresholds are lower and dorsal horn cutaneous receptive are poorly tuned. Spinal inhibitory systems appear to mature slowly over the first postnatal weeks. The two major inhibitory neurotransmitters in the spinal cord are GABA and glycine. We have previously shown that GABA signalling is fully functional in the newborn cord (1), but the role of glycine in development has not been fully investigated. In the adult spinal dorsal horn cells in lamina (L) III-VI are under tonic glycinergic control and intrathecal (i.t.) strychnine, a specific glycine receptor antagonist, induces spontaneous pain and sensitization to mechanical stimuli (2). Glycinergic neurons receive monosynaptic input from both low threshold myelinated and nociceptive afferents acting as a negative feedback to excitatory neurones in the dorsal horn. Whole cell patching of LII neurons in newborn spinal cord slices revealed an absence of glycinergic mIPSCs and little or no afferent evoked glycinergic activity, despite the presence of functional glycine receptors from birth (3). The aim of this study was to undertake an in vivo analysis of the functional maturation of glycinergic synaptic transmission in the spinal dorsal horn and establish the role of glycinergic signalling in the postnatal organisation of dorsal horn circuits. Spontaneous and brush-evoked responses of individual dorsal horn neurons were recorded extracellularly in isoflurane gas-anaesthetised rats (1.8% in O_2), and strychnine applied to the surface of the exposed cord. Glycinergic activity was also examined by quantifying the change in fos expression in the dorsal horn 20 minutes following i.t. strychnine with and without brush stimulation of the hind paw. Immunostaining for GlyT2 (1:40,000, kind gift from Professor F Zafra) was used to map the distribution of glycinergic terminals in the developing dorsal horn. Spontaneous activity of spinal dorsal horn neurons increased in postnatal day (P)21 rats following strychnine (mean increase 0.26±0.16 spikes/sec (SEM) from baseline, P= 0.01, non-parametric ttest) but had no effect on that of P3 dorsal horn neurons. Brush-evoked activity increased markedly in mature neurons 20 minutes post strychnine (mean increase 6.61±1.81 spikes/sec, $P<0.05$) but was inhibited in P3 neurons (mean decrease 2.17±0.73 spikes/sec, $P<0.05$). Fos expression mirrored in vivo findings, with no apparent increase in activated neurons following strychnine in the neonatal dorsal horn. GlyT2 staining revealed an absence of glycinergic terminals in the superficial dorsal horn at P3, with gradual appearance in LIII by the P21. From these results, we can conclude that specific glycinergic inhibition of low threshold afferent sensory evoked activity is absent in neonatal dorsal horn circuits and the primary role of glycinergic transmission in the early postnatal period is to facilitate transmission of sensory input.

Bremner L et al (2006) J Neurophysiol (6): 3893-7.

Sivilotti L, Woolf CW (1994) J Neurophysiol (72): 169-79.

Baccei ML, Fitzgerald M (2004) J Neurosci (24): 4749-57.

MRC.

Where applicable, the authors confirm that the experiments described here conform with The Physiological Society ethical requirements.

C06

Representation of temporal sensory features in the whisker thalamus

R. Petersen[1], M. Bale[1], A. Alenda[2], M. Brambilla[1], S. Panzeri[3], M. Montemurro[1] and M. Maravall[2]

[1]Faculty of Life Sciences, University of Manchester, Manchester, UK, [2]Instituto de Neurociencias, UMH-CSIC, Alicante, Spain and [3]Italian Institute of Technology, Genoa, Italy

The thalamo-cortical pathway is the crucial sensory gateway into the cerebral cortex. We aimed to determine both the nature of the tactile information encoded by neurons in the

whisker somatosensory relay nucleus (VPm) and how it is encoded. We wanted to distinguish whether VPm neurons encode similar stimulus features, acting as a single information channel, or encode diverse features. We also wanted to determine whether stimulus features are encoded by the firing rate or by the precise timing of spikes.

To address these issues, we recorded responses of single units in the rat VPm under urethane anaesthesia (i.p., 1.5 g (kg bodyweight)$^{-1}$) to whisker deflections that thoroughly explored the space of temporal stimulus variables (for experimental details, see Montemurro et al., 2007). We then identified features to which neurons were selective by reverse correlation. We found that spikes were timed with sub-millisecond precision, and that this enabled neurons to convey a great deal of information (up to 77.9 bits/s) about whisker motion. To identify which sensory features these precisely timed spikes encode, we used a reverse correlation approach. We found that sensitivity to stimulus kinetics was surprisingly diverse. Some neurons (25%) only encoded velocity; others were sensitive to position, acceleration or more complex features. A minority (19%) encoded two or more features. These results indicate that VPm contains a distributed representation of whisker motion, based on high-resolution kinetic features.

Bale M.R., Petersen R.S. (in press) Transformation in the neural code for whisker deflection direction along the lemniscal pathway. J. Neurophysiol.

Montemurro M., Panzeri S., Maravall M., Alenda S., Bale M., Brambilla M. and Petersen R.S. (2007) Role of precise spike timing and correlated spike patterns in coding of dynamic vibrissa stimuli in somatosensory thalamus. J. Neurophysiol. 98: 1871-1882.

Petersen R.S., Brambilla M., Bale M.R., Alenda A., Panzeri S., Montemurro M.A., Maravall M. (2008) Diverse and temporally precise kinetic feature selectivity in the VPm thalamic nucleus. Neuron 60: 890-903.

Funded by BBSRC and EPSRC (CARMEN e-science project).

Where applicable, the authors confirm that the experiments described here conform with The Physiological Society ethical requirements.

C07

Pharmacological modulation of oscillatory local field potentials in the accessory olfactory bulb of anaesthetised mice

E. Leszkowicz and P. Brennan

Department of Physiology and Pharmacology, University of Bristol, Bristol, UK

Synaptic changes in the accessory olfactory bulb (AOB) have been proposed to underlie the ability of female mice to learn the chemosensory signature of their mate at mating. Mate recognition is vital for reproductive success and is thought to involve a learning-induced increase in feedback inhibition, which selectively gates the transmission of the learned signal at the level of the AOB[1]. The tight coupling between excitatory projection neurons and inhibitory interneurons, at dendrodendritic reciprocal synapses, produces synchronized neural activity that is evident in the oscillatory local field potential (LFP) recorded in the AOB. Our aim was to investigate whether changes in the balance of excitatory and inhibitory neurotransmission could affect the oscillatory dynamics of AOB activity, with the potential to affect functional coupling with other brain areas[2].

Mice were anaesthetised by intraperitoneal injection of urethane (1.6g/kg body weight, 22% urethane) and a bipolar recording electrode, with integral drug delivery cannula, was inserted in the mitral/tufted cell layer of the AOB. LFP power and dominant frequencies in different frequency bands were analysed pre-infusion and following a 1μl infusion of either drug or artificial cerebrospinal fluid (CSF) at intervals up to 1 hour post-infusion. Infusions of 100pmol of the type II metabotropic glutamatergic receptor agonist DCG-IV (n=4), or 1nmol of the $GABA_A$ receptor agonist isoguvacine (ISO, n=5) resulted in a significant and lasting reduction in power in bands between 4 and 90Hz, compared to CSF (n=4) (Tukey post-hoc multiple comparisons test: DCG-IV: p=0.002 (4-12Hz), p=0.001 (12-30, 60-90Hz); ISO: p<0.001 (4-12, 12-30Hz), p=0.003 (60-90Hz)). This effect is consistent with a direct inhibition of excitatory neurons by isoguvacine and a pre-synaptic inhibition of glutamate release by DCG-IV. Infusion of 0.5ng of the $GABA_A$ antagonist gabazine (n=5), which would be expected to disinhibit the excitatory neurons, failed to have a significant effect on the power of LFP oscillations. This might be explained by the dose of gabazine being too low, but increases in the dose to 2ng resulted in epileptiform-like activity that precluded analysis. Surprisingly, none of the drugs significantly affected the dominant frequency of oscillatory activity in any of the frequency bands. This suggests that the frequency of oscillatory neural activity in the AOB might be more dependent on aspects of neural connectivity rather than the balance between excitatory and inhibitory neurotransmission. This finding would support the hypothesis that the gating of learned vomeronasal information at the level of the AOB may occur through direct inhibition of mitral/tufted projection neuron activity rather than by a decoupling of neural oscillators in the AOB and central brain areas[2].

1. Brennan PA & Zufall F (2006). *Nature* **444**, 308-315.

2. Taylor JG & Keverne EB (1991). *Biol Cybern* **64**, 301-306.

This work was funded by BBSRC grant BB/E020283/1.

Where applicable, the authors confirm that the experiments described here conform with The Physiological Society ethical requirements.

C08

Widespread activation of the thalamo-cortical visual pathway by melanopsin photoreceptors

T.M. Brown[1], C. Gias[2], M. Semo[2], P.J. Coffey[2], J. Gigg[1], H.D. Piggins[1] and R.J. Lucas[1]

[1]Faculty of Life Sciences, University of Manchester, Manchester, UK and [2]Institute of Ophthalmology, University College London, London, UK

A subset of retinal ganglion cells, that express melanopsin, are intrinsically photosensitive (ipRGCs). Activity of these ipRGCs defines responses to environmental irradiance such as circadian photoentrainment and the pupil light reflex, but a role in image-forming vision has been widely discounted since projections to the dorsal lateral geniculate (dLGN; thalamic relay

to the visual cortex) have not been observed. Since it has now clear that the marker used to track ipRGC projections in earlier studies only labels ~50% of ipRGCs, we revisited the possibility that ipRGCs contribute to image-forming visual processing. We investigated how melanopsin signals influenced neural activity in the visual thalamus using multichannel extracellular recordings in urethane anaesthetised mice (1.7g/kg). In mice lacking rods and cones (*rd/rd cl*), full field illumination of the contralateral eye (460±10nm) evoked excitatory responses in a large proportion (~40%, n=1051) of cells throughout the ventral and dorsal LGN. To determine whether this widespread appearance of melanopsin signals in the LGN reflected compensatory changes in *rd/rd cl* mice, we turned to red cone knockin mice (*Opn1mw*^{R}). These animals have a fully intact retina, but cone-dependent responses can be identified by their anomalous sensitivity to red light. In these mice, all light-responsive cells (n=248) showed rod/cone mediated transient changes in spike rate at light on/off. However, almost half of these cells also exhibited sustained responses to 60s bright light that could not have been mediated via rods or cones. To confirm that these sustained responses originated with melanopsin we used melanopsin knockout mice. LGN neurons in these animals maintained robust transient responses at light on/off (n=217), however, unlike cells in *rd/rd cl* and *Opn1mw*^{R} mice, were unable to sustain elevated firing rates throughout a 60s stimuli. Finally we used intrinsic optical imaging to determine whether these melanopsin signals evident in the dLGN were conveyed to higher visual centres. We found a robust light-activation of V1, V2M and retrosplenial cortex in *rd/rd cl* mice that was almost identical to that of wild-type (both n=6) at all but the shortest timescales. In conclusion, our data indicate that the thalamo-cortical visual pathway is a principal target of melanopsin photoreception.

This work was funded by the Wellcome Trust and was supported in part by the London Project to Cure Blindness.

Where applicable, the authors confirm that the experiments described here conform with The Physiological Society ethical requirements.

C09

Acceleration of ocular dominance plasticity by H-Ras activation in developing visual cortex

C.E. Cheetham[1], M. Kaneko[2], A.J. Silva[3], M.P. Stryker[2] and K.D. Fox[1]

[1]School of Biosciences, Cardiff University, Cardiff, UK, [2]Department of Physiology, UCSF, San Fransisco, CA, USA and [3]Department of Neurobiology, Psychology, Psychiatry and the Brain Research Institute, UCLA, Los Angeles, CA, USA

H-Ras/extracellular signal-related kinase (ERK) signaling has been shown to modulate hippocampal learning and plasticity (1). ERK signalling has also been implicated in both ocular dominance plasticity and long-term potentiation (LTP) in developing visual cortex (2).To investigate the role of H-Ras in plasticity in developing visual cortex, we used transgenic mice expressing constitutively active H-Ras (H-Ras^{G12V}) at levels similar to endogenous H-Ras. We examined the effects of monocular deprivation (MD) on responses in primary visual cortex (V1) during the critical period for ocular dominance plasticity (post-natal day 24-30) using chronic intrinsic signal imaging. Monocular deprivation (3) was performed by suturing the right eye shut under isoflurane anaesthesia (3% in O_2). For imaging (4), mice were anaesthetised with isoflurane (0.8% in O_2) and 25μg chlorprothixene I.M. We used repeated measures ANOVAs to assess longitudinal changes and one-way ANOVAs to compare genotypes. During MD in wild-type (WT) mice (n=5), an initial depression of closed eye responses is evident after 3 days (-28±3%, mean±S.E.M., P<0.001), followed by a delayed increase in open eye responses after 6 days (+36±2%, P<0.001). In H-Ras mice (n=6), depression of closed eye responses was comparable to that in WT mice after 3 days' MD (-26±4, P>0.05), but plasticity of open eye responses was dramatically accelerated, showing a large increase after 3 days' MD (+20±3%, P<0.001 vs baseline, P<0.05 vs WT). To investigate the cellular mechanisms underlying this accelerated plasticity, we made whole cell recordings from layer 2/3 (L2/3) pyramidal neurons in V1 in acute brain slices. LTP at L4 to L2/3 synapses was enhanced in H-Ras mice: mean LTP magnitude 1 hour post-induction was 11±1% in WT and 56±13% in H-Ras mice (P=0.046, t-test, n=15/group). L4 to L2/3 synapses also showed greater short-term facilitation in H-Ras mice (paired pulse ratio (PPR): 1.02±0.03 in WT, 1.22±0.05 in H-Ras, P=0.002, t-test, n=20/group). Moreover, 1 hour after LTP induction, PPR was decreased significantly in H-Ras mice (from 1.42±0.08 to 1.15±0.04, P=0.001) but not in WT mice (from 1.25±0.06 to 1.23±0.12, P=0.69, paired t-tests), suggesting that altered presynaptic release at least partially accounts for enhanced LTP. Therefore, we directly compared presynaptic release probability in H-Ras and WT mice using the rate of use-dependent blockade of NMDARs (N-methyl-D-aspartate receptors) by MK-801. NMDARs blocked more slowly in H-Ras than WT mice (55±15 vs 16±5 trials to reach 50% block, P=0.026, t-test, n=10/group), indicating that release probability is lower in H-Ras mice. Our data indicate that H-Ras activation reduces presynaptic release probability at developing visual cortex synapses. This may underlie the enhanced LTP and accelerated ocular dominance plasticity that we describe.

Kushner SK *et al.* (2005). *J Neurosci* **25**, 9721-34.

Di Cristo G *et al.* (2001). *Science* **292**, 2337-40.

Gordon JA & Stryker MP (1996). *J Neurosci* **16**, 3274-86.

Kaneko M *et al.* (2008). *Nat Neurosci* **11**, 497-504.

Funded by the NIMH

Where applicable, the authors confirm that the experiments described here conform with The Physiological Society ethical requirements.

C10

Single dendrite directional selectivity in neocortical pyramidal neurons, assisted by NMDA spikes and excitatory-inhibitory interactions

G. Major and K.D. Fox

School of Biosciences, Cardiff University, Cardiff, Wales, UK

Many neurons in sensory areas of the brain are directionally selective. In visual cortex, cells commonly fire more in response

to oriented light or dark bars sweeping in one direction compared with the reverse[1]. Analogous directionality is seen in somatosensory[2] and auditory cortex. The mechanisms are still debated. In retina and some invertebrate systems, local dendritic computations support directionality: could this play a role in mammalian neocortex?

Most inputs into cortical neurons arrive on sub-micron diameter "thin" dendrites, such as basal & apical oblique dendrites, which can also fire NMDA spikes in response to sufficient excitatory synaptic stimulation[3]. NMDA spikes are ideally suited to the computation of directionality:

a) Focally-evoked NMDA spikes in basal & oblique dendrites exhibit pronounced spatial gradients in both amplitude & glutamate threshold[4]: a proximal NMDA spike can produce a 7-fold bigger somatic voltage swing than a distal NMDA spike in the same dendrite & requires ~5 times as much glutamate to cross threshold (in large layer 5 cells).

b) Depolarisation reduces the glutamate threshold for an NMDA spike: a distal NMDA spike can help a more proximal one in the same dendrite cross threshold (co-operativity)[4].

Simulations predict these features should allow single dendrites to generate bigger responses following distal-to-proximal (DP) sweeps of glutamate stimuli compared with exactly the same stimuli in proximal-to-distal (PD) order; also, strategically placed and timed inhibition should enhance this directionality.

To test this, combined whole-cell recording, 2-photon Ca^{2+} imaging, patterned 2-photon glutamate uncaging[5] and focal GABA iontophoresis experiments were performed on layer 5 pyramidal cells in rat somatosensory cortical slices. Single basal and oblique dendrites were stimulated with sweeps of glutamate spots in both directions (≤90 x 0.5-1 ms uncaging spots near spines, sweep duration <230 ms), in ~½ of cases comparing responses with/without 5 ms GABA pulses onto the proximal part of the same dendrite. Single dendrites could exhibit up to 7-fold or more directionality (DP response/PD response); average maximum achieved directionality of each dendrite = 2.84 ± 1.73 (mean ± sd; range 1.3-8.8, n=21 dendrites with >100 μm stimulated; no action potentials). Directionality depended on sweep speed, baseline voltage & spatial pattern of stimuli, & increased with length stimulated. Directionality was enhanced by proximal inhibition before PD sweeps (IPD), but after DP sweeps (DPI). This increased:

a) the range of stimuli giving directionality,

b) the directionality of a given excitatory pattern (1.62±1.07-fold mean increase per pattern, n=39 patterns).

Over 11 dendrites, the maximum enhancement of directionality by inhibition averaged 1.84±1.07-fold (range 1.1-4.2).

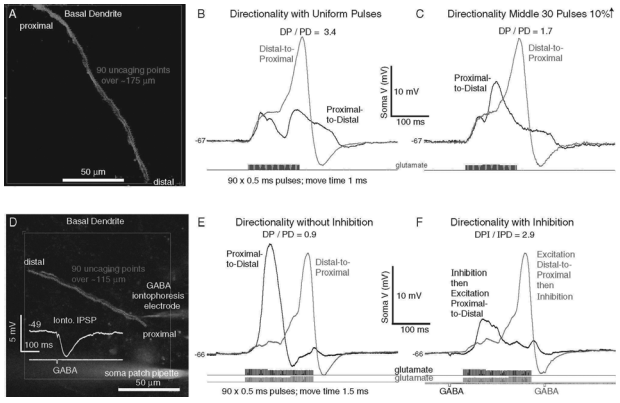

Figure 1. Examples of directionally-selective responses to patterned uncaging sweeps of glutamate spots. Top: excitation alone. Directionality sensitive to exact stimulus pattern. Bottom: timed proximal inhibition (brief iontophoretic GABA pulse) can enhance directionality.

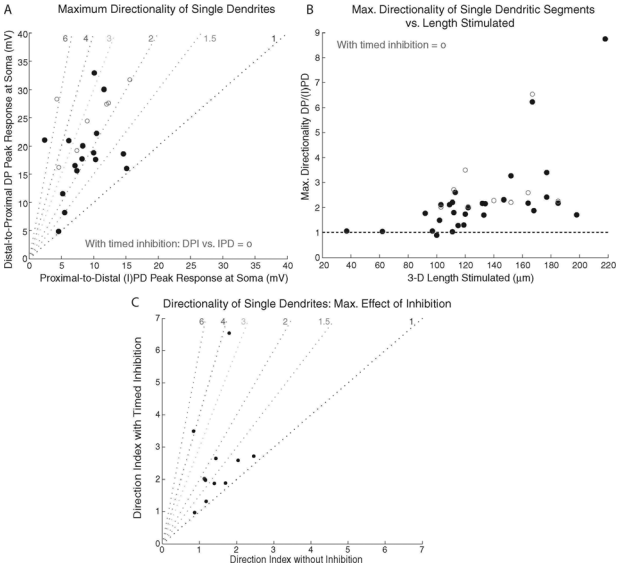

Figure 2. A. Maximum directionality of different dendrites. Red circles = cases with timed inhibition giving biggest directionality. B. Maximum directionality vs. length of segment stimulated. C. Maximum effect of timed inhibition on directionality of 11 dendrites tested with glutamate sweeps +/- GABA pulse.

Hubel, D.H. & Wiesel, TN (1959). Receptive fields of single neurones in the cat's striate cortex. J Physiol 148, 574-91.

Jacob, V, Le Cam, J, Ego-Stengel, V & Shulz, DE (2008) Emergent properties of tactile scenes selectively activate barrel cortex neurons. Neuron 60, 1112-25.

Schiller J, Major G, Koester HK and Schiller I (2000). NMDA spikes in basal dendrites of cortical pyramidal neurons. Nature 404, 285-289.

Major G, Polsky A, Denk W, Schiller J, Tank DW (2008). Spatio-temporally graded NMDA spike/plateau potentials in basal dendrites of neocortical pyramidal neurons. J. Neurophysiol. 99, 2584-601.

Losonczy, A & Magee, JC (2006). Integrative Properties of Radial Oblique Dendrites in Hippocampal CA1 Pyramidal Neurons. Neuron 50, 291-307.

BBSRC

Where applicable, the authors confirm that the experiments described here conform with The Physiological Society ethical requirements.

C11

Experience-dependent plasticity and spontaneous activity depend on cell identity in layer V of the barrel cortex

V. Jacob, N. Wright and K.D. Fox

School of Biosciences, Cardiff University, Cardiff, UK

Experience dependent plasticity (EDP) has mainly been studied in layers II/III and IV of barrel cortex to date and little is known of layer V EDP. Layer V contains a relatively heterogeneous population of neurons including intrinsic bursting (IB) and regular spiking (RS) cells as well as sublaminae Va and Vb. Previous studies have suggested that sub-types of layer V pyramidal cells show different levels of spine plasticity (Holtmaat et al., 2006). To test whether functional plasticity was also different between sub-types of pyramidal cells we performed single-row whisker deprivation lasting 0, 3 or 10 days in 6 week old rats and recorded both evoked and spontaneous activity with extracellular carbon fiber or intracellular sharp electrodes in layer Va and Vb of the deprived barrel columns under urethane anesthesia (1.5 g/kg, I.P. injection).

We classified intracellularly-recorded neurons as RS and IB cells. We investigated whether some properties of the spontaneous activity could be used to reveal the intrinsic properties of the cells. Firstly, we did not find any obvious relationship between the timing of the spikes in a spontaneous train and the intrinsic properties of the cells. Secondly, we observed that the ratio between the amplitude of the second spike vs. the first spike in a pseudo-burst (inter-spike interval below 10 ms) is significantly smaller for IB cells (mean ± SD: 0.72 ± 0.12) than for RS cells (0.90 ± 0.10, Student's unpaired t-test $p<0.005$).

After 3 days and 10 days of deprivation, we observed trough extracellular recordings a depression of the deprived principal whisker and a potentation of the spared whiskers in both layers Va and Vb. We calculated the spike amplitude ratio only for the best discriminated pseudo-bursts during spontaneous activity. Following deprivation, we found a link between the shape of the receptive field and the spike amplitude ratio. For 3 days but not 0 days of deprivation, the response to stimulation of the principal whisker is positively correlated in layer Va ($r2 = 0.19$, $P<0.01$) and negatively correlated in layer Vb ($r2 = 0.15$, $P<0.05$) with the spike amplitude ratio. The depression is cell-type and sublaminae-dependent. In both layers Va and Vb, the response to the best spared whisker is positively correlated with the spike amplitude ratio after 10 days of deprivation (layer Va, $r2 = 0.97$, $P<0.0005$; layer Vb, $r2 = 0.28$, $P<0.001$) but not after 3 days. The potentiation is more pronounced for RS-like cells than for IB-like cells.

Our results suggest that sensory deprivation differentially affects the subclasses of neurons in layer V of the barrel cortex. This observation could result either from differences in the input patterns or from different intrinsic mechanisms for inducing plasticity in different sublaminae and subtypes of layer V pyramidal neurons.

Holtmaat et al. (2006). Nature 441(7096), 979-83

We thank the MRC and NIH for funding.

Where applicable, the authors confirm that the experiments described here conform with The Physiological Society ethical requirements.

C12

Rapid, learning-induced inhibitory synaptogenesis in murine barrel field

S. Glazewski[1], M. Jasinska[2], E. Siucinska[3], A. Cybulska-Klosowicz[3], E. Pyza[2], D.N. Furness[1] and M. Kossut[3]

[1]School of Life Sciences, Keele University, Keele, UK, [2]Institute of Zoology, Jagiellonian University, Krakow, Poland and [3]The Nencki Institute, Warsaw, Poland

The structure of neurones changes during development and in response to injury or alteration in sensory experience. Changes occur in the number, shape and dimensions of dendritic spines together with their synapses. However, precise data on these changes in response to learning are sparse. Here, after a period of habituation, mice were conditioned according to classical (Pavlovian) paradigm. A stroke of the selected whisker (CS) on one side of the snout was paired with a mild tail shock (UCS) (Siucinska & Kossut, 1996). We show using quantitative transmission electron microscopy (TEM) that a simple form of learning involving mystacial vibrissae in mice results in about 70% increase in the density of inhibitory synapses on spines of neurones located in layer IV barrels that represent the stimulated vibrissae (control, 0.27 SD ± 0.05 per μm3 versus conditioned, 0.47 ± SD 0.09 per μm3; ANOVA, $p<0.001$, $F= 14.94$, total $df=27$). The spines contain one asymmetrical (excitatory) and one symmetrical (inhibitory) synapse (double-synapse spines) and their density increases 3-fold due to learning with no apparent change in the density of asymmetrical synapses (control, 0.10 ± 0.03 versus conditioned, 0.29 ± 0.07 per μm3; ANOVA, $p<0.001$, $F=18.95$, total $df=27$). This effect seems to be specific for learning as pseudoconditioning (where the conditioned and unconditioned stimuli are delivered at random) does not lead to the enhancement of symmetrical synapses, but instead results in an up-regulation of asymmetrical synapses on spines (controls, 1.19 SD ± 0.15 per μm3 versus pseudo-conditioned, 2.34 SD ± 0.62 per μm3; ANOVA, $p<0.001$, $F=14.46$ and total $df=27$). Symmetrical synapses of cells located in barrels receiving the conditioned stimulus show also a greater concentration of γ-amino-butyric acid (GABA) in their presynaptic terminals as measured with immunogold histochemistry under the TEM (control,12.31 gold particles per μm2 ± SE 3.59 versus conditioned, 27.06 gold particles per μm2 SE ± 4.83; Mann-Whitney, $p<0.0001$, 3 animals per group; control, 147 symmetrical terminals counted versus conditioned, 153 symmetrical terminals counted). These results indicate that the immediate effect of classical conditioning in the 'conditioned' barrels is rapid, pronounced and inhibitory.

Siucinska E & Kossut M (1996). Cereb Cortex 6, 506-513.

This work was supported by a Wellcome Trust Grant to S.G. and M.K., Royal Society and Physiological Society grants to S.G. and grants from the Erasmus and Sie ć BW/IZ/72/2007 to M.J.

Where applicable, the authors confirm that the experiments described here conform with The Physiological Society ethical requirements.

C13

Neurons in the rostral ventromedial medulla (RVM) that possess the NK-1 receptor contribute to descending facilitation of spinal nociceptive transmission

S.G. Khasabov and D.A. Simone

Diagnostic and Biological Sciences, University of Minnesota, Minneapolis, MN, USA

Activation of neurokinin-1 receptors (NK-1R) in the spinal cord by substance P (SP) released from nociceptive afferent fibers contributes to central sensitization and hyperalgesia. Neurons possessing NK-1R are also found in the RVM, an area of the brainstem that gives rise to descending modulation of nociceptive transmission in the spinal cord. It has been suggested that RVM neurons with NK-1R contribute to descending facilitation of pain. We therefore investigated the effects of ablation of RVM neurons with NK-1R on acute pain, development of hyperalgesia, and sensitization of spinal neurons.
To eliminate NK-1R expressing neurons, the ribosomal toxin Saporin (SAP) conjugated to the SP stable analog $Sar^9,Met(O_2)^{11}$-Substance P (SSP-SAP; 1 μM/0.5 μl) or Blank-SAP (control) was injected into the RVM of Sprague Dawley rats under i.p. ketamine anesthesia. At 14-28 days after injection, SSP-SAP reduced the number of NK-1R positive neurons in the RVM (0.3% ± 0.16% of all neurons) compared to Blank-SAP (7.1% ± 1.05%) and naïve (6.8% ± 0.57%) rats (one-way ANOVA, $p<0.001$).
SSP-SAP did not alter the frequency of paw withdrawal, evoked by a 15g von Fray monofilament, or paw withdrawal threshold. However, SSP-SAP produced a 50% decrease in the duration of nocifensive behavior following intraplantar injection of capsaicin ($p<0.001$, t-test) and decreased the magnitude of mechanical hyperalgesia.
To determine whether activation of NK-1R in the RVM are involved in sensitization of nociceptive neurons in the spinal cord, we examined the effects of injection of the NK-1R antagonist L-733,060 (1.5 pmol/0.5μl) or vehicle into the RVM on electrophysiological responses of spinal neurons in rats anesthetized with i.v. Nembutal. The NK-1R antagonist reduced responses evoked by capsaicin and the ensuing sensitization to mechanical stimuli ($p<0.05$; one- and two-way repeated measures AVOVA). These results were consistent with our previous behavioral studies in which injection of L-733,060 into the RVM decreased the duration of nocifensive behaviors and mechanical hyperalgesia produced by capsaicin.
We also determined whether activation of NK-1R in the RVM produced hyperalgesia. Injection of the NK-1R agonist $Sar^9,Met(O_2)^{11}$-Substance P (SSP) (0.1-10 nmol/0.5 μl) into the RVM reduced paw withdrawal threshold at doses of 3, 5, and 10 nmol ($p<0.05$; two-way repeated measures AVOVA). Withdrawal thresholds decreased by approximately 5-6 g.
We conclude that neurons in the RVM that possess NK-1 receptors have a unique role in descending facilitation of spinal nociceptive transmission and hyperalgesia evoked by capsaicin. These neurons in the RVM do not appear to modulate acute pain.

Supported by NIH grants CA91007, DA11471 and DA023576, and a grant from the Graduate School of the University of Minnesota.

Where applicable, the authors confirm that the experiments described here conform with The Physiological Society ethical requirements.

C14

Modulation of the monosynaptic H-reflex by the periaqueductal grey

S. Koutsikou, L. Brock, O. Ruscombe-King, B.M. Lumb and R. Apps

Department of Physiology & Pharmacology, University of Bristol, Bristol, Bristol, UK

Outputs from the different functional columns in the periaqueductal grey (PAG) evoke different patterns of co-ordinated motor responses associated with active or passive coping. Active coping is elicited by the dorsolateral/lateral (dl/l) PAG and enables an animal to escape a stressor. It is also characterised by increased mobility (flight or fight behaviours). In contrast, passive coping is elicited by the ventrolateral (vl) PAG and is characterised by cessation of movement and a tense posture.
Very little is known about how the PAG influences spinal reflex circuits that contribute to the above repertoire of motor responses. As a first step, the aim of the present study was to examine the effects of neuronal activation in dl/lPAG versus vlPAG on motoneuronal excitability. Specifically, the H-reflex was used as a 'motor readout' to measure changes in α-motoneurone excitability during PAG activation.
In alphaxalone-anaesthetised (i.v. Alfaxan, Jurox; $25mg.kg^{-1}.hr^{-1}$) adult rats (n=14), H-reflex responses were evoked in the hindlimb plantaris muscle by electrical stimulation of the left tibial nerve using subcutaneous needle electrodes inserted at the level of the ankle joint (stimulation rate was once every 6s and the stimulus duration was 0.5ms cf. Gozariu et al. 1998). The H-reflex responses were examined before and following neuronal activation with 50mM DL-homocysteic acid microinjections (max.100nl) in either the ipsilateral dl/l or vlPAG.
Activation in the vlPAG significantly increased the amplitude of the H-reflex by 88±11.4% ($P<0.001$, n=9). In contrast, dl/lPAG activation did not alter the H-reflex significantly ($P>0.05$, n=5). In the same experiments the M response was used as a control for constancy of the electrical stimulus and for both dl/l and vl PAG activation the M response remained unchanged ($P>0.05$, n=5 and n=9, respectively).
The data reveal differential descending control exerted by the PAG on the excitability of α-motoneurones, which we suggest could contribute to different coping behaviours co-ordinated by the vlPAG.

Gozariu M et al. (1998) Brain Res 782:343-347.

Supported by the BBSRC.

Where applicable, the authors confirm that the experiments described here conform with The Physiological Society ethical requirements.

C15

Midbrain control of spinal cold processing

J. Leith, S. Koutsikou, B.M. Lumb and R. Apps

Department of Physiology & Pharmacology, University of Bristol, Bristol, UK

Peripheral mechanisms of cold somatosensation in normal and pathophysiological states have received much recent interest. However, information about the central processing of cold sensory input is lacking, particularly whether these inputs may be modulated by descending control systems that have profound effects on the processing of other sensory modalities. This study characterised spinal responses to low and high intensity cold stimuli and established the extent to which they are modulated by descending control from the periaqueductal grey (PAG), a major determinant of acute and chronic pain.

In alphaxalone-anaesthetised (Alfaxan; 15-30mg.kg-1.hr-1, i.v.) male Wistar rats (280-300g) either paw withdrawal reflexes (measured as EMG activity from biceps femoris; n=5) or extracellular neuronal activity from lumbar spinal dorsal horn neurones (32 cells, from n=19) was recorded in response to hindpaw cooling with acetone and ethyl chloride (both 1ml topically).

Ethyl chloride, but not acetone, produced sufficiently noxious cold to evoke withdrawal reflexes in lightly anaesthetised rats, which were significantly depressed ($p<0.01$, ANOVA) by chemical stimulation of the ventrolateral (VL)-PAG with D,L-homocysteic acid (DLH, 80nl, 50mM in physiological saline saturated with pontamine sky blue dye to mark injection sites).

Dorsal horn neurones were characterised according to their responses to low (brush, tap) and high (pinch) threshold mechanical stimulation applied to the receptive field and classified as class 1 (low threshold), class 2 (wide dynamic range) and class 3 (nociceptive-specific; Menetrey et al, 1977). Cells were then tested for thermal responses with acetone, ethyl chloride and noxious heat. The majority of class 1 and 2 cells responded to both acetone and ethyl chloride (66 & 85% respectively), in contrast to only around half (55%) of class 3 cells. The effects of VL-PAG stimulation were tested in cold responsive cells, which produced differential effects on cold responses dependent on cell type and stimulus intensity. All cold-evoked activity in non-nociceptive class 1 cells and innocuous cold (acetone) responses of class 2 neurones remained unaltered (n=3-6; all $p>0.05$, ANOVA). In contrast, noxious cold (ethyl chloride) responses of class 2 neurones and all cold-evoked activity in nociceptive-specific class 3 neurones were significantly depressed (n=3-7; all $p<0.01$, ANOVA).

The data demonstrate that spinal responses to noxious cold can be powerfully modulated by descending control systems originating in the PAG, and suggests that this control is selective for noxious versus innocuous stimulus intensities.

Menetrey et al (1977) Exp Brain Res 27(1):15-33.

Funding from BBSRC.

Where applicable, the authors confirm that the experiments described here conform with The Physiological Society ethical requirements.

C16

Brief sacral nerve root stimulation and tibial nerve stimulation increases cortical somatosensory evoked potential in the rat

K.M. Griffin[1], C. O'Herlihy[2], R. O'Connell[3] and J.F. Jones[1]

[1]School of Medicine and Medical Science, University College Dublin, Dublin 4, Ireland, [2]National Maternity Hospital, Holles Street, Dublin 2, Ireland and [3]Academic Surgical Unit, St Vincent's University Hospital, ElmPark, Dublin 4, Ireland

Faecal incontinence in women is associated with pudendal nerve damage sustained during traumatic childbirth (Snooks et al. 1984). Sacral nerve stimulation (SNS) and tibial nerve stimulation (TNS) are used as treatments for this condition. SNS has been employed as a therapy since 1995 (Matzel et al. 1995), but it is quite invasive and costly. Recently clinical trials have taken place using TNS as a treatment for faecal incontinence. There are a small number of trials using TNS, but the results to date have been promising (Mentes et al. 2007; Queralto et al. 2006; Vitton et al. 2009). The exact mechanism of action of SNS or TNS remains unclear. It is possible that affected individuals with pudendal nerve damage develop a sensory deprivation syndrome and that sacral neuromodulation increases the sensory input to the cortex. The aim of this experiment was to study evoked potential following anal canal stimulation before and after acute SNS and TNS.

Twenty one female virgin Wistar rats (body mass: 200-250g) were used. Three groups were constructed, group 1: control, group 2: SNS and group 3: TNS. Animals were anaesthetised with urethane (1.5g/kg i.p.). The femoral artery and vein were cannulated and the animals were ventilated with supplemental O2. Arterial blood gases and respiration rate were monitored thoughout the experiment. A unilateral craniotomy was performed over the right hemisphere. An extradural recording array (FlexMEA, multi-channel systems) was placed over the right somatosensory cortex. A cathode placed in the anal canal was used to provide triggered stimulation at 1Hz (amplitude: 10volts and pulse duration 0.1ms). Four trials of 500 sec sweeps were recorded in each group. Following the first trial in group 2, SNS was applied (amplitude: 6 volts, frequency 15Hz and duration 1ms) and in group 3, TNS (amplitude: 20 volts, frequency 15Hz and duration 1ms). After stimulation 3 consecutive trials were run. In all groups the amplitude of the first trial was designated 100%, each trial was normalised against this.

The amplitude of the somatosensory evoked potential in group 1 was stable over all four trials. Following the application of SNS in group 2, there was an increase in amplitude from 100% to 158.9 ± 10.60%. This amplitude increase was sustained in all 3 trials following SNS. Group 3 also resulted in an increase in amplitude following TNS, the SEP increased from 100 % to 148.1 ± 22.56% following stimulation. As seen in group 2, the amplitude increase following stimulation to the tibial nerve remained constant until the conclusion of the experiment.

The findings support the hypothesis that even brief SNS and TNS can increase sensory input from the anal canal to the somatosensory cortex. These results indicate a similar mechanism of action of both therapies.

Matzel KE, Stadelmaier U, Hohenfellner M, and Gall FP. Electrical stimulation of sacral spinal nerves for treatment of faecal incontinence. Lancet 346: 1124-1127, 1995.

Mentes BB, Yuksel O, Aydin A, Tezcaner T, Leventoglu A, and Aytac B. Posterior tibial nerve stimulation for faecal incontinence after partial spinal injury: preliminary report. Tech Coloproctol 11: 115-119, 2007.

Queralto M, Portier G, Cabarrot PH, Bonnaud G, Chotard JP, Nadrigny M, and Lazorthes F. Preliminary results of peripheral transcutaneous neuromodulation in the treatment of idiopathic fecal incontinence. Int J Colorectal Dis 21: 670-672, 2006.

Snooks SJ, Setchell M, Swash M, and Henry MM. Injury to innervation of pelvic floor sphincter musculature in childbirth. Lancet 2: 546-550, 1984.

Vitton V, Damon H, Roman S, Nancey S, Flourie B, and Mion F. Transcutaneous posterior tibial nerve stimulation for fecal incontinence in inflammatory bowel disease patients: a therapeutic option? Inflamm Bowel Dis 15: 402-405, 2009.

Health research board Ireland.

Where applicable, the authors confirm that the experiments described here conform with The Physiological Society ethical requirements.

C17

Competing changes in evoked activity in a polysensory brain region during imprinting in domestic chicks

A. Nicol[1] and G. Horn[2]

[1]Laboratory of Cognitive and Behavioural Neuroscience, Babraham Institute, Cambridge, UK and [2]Subdepartment of Animal Behaviour, University of Cambridge, Cambridge, UK

Imprinting is a process whereby a domestic chick comes to recognise a conspicuous object by being exposed to it. Experimentally, 14 visually naive chicks were presented with a compound training stimulus (TC) during two 1h periods. The TC was a rotating, internally illuminated visual object (Tvis), a red box or blue cylinder, and a simultaneously presented recording of a maternal call (MC). Action potential activity (spikes) was recorded from the intermediate medial mesopallium (IMM), a polysensory area in the chick forebrain, that is a store for the memory underlying imprinting (1). Through imprinting, the proportion of IMM neurons responding to the visual imprinting stimulus increases dramatically, and non-linearly (2). Here we examine the effects of training on IMM neuron responses to the TC, and to its separate components, the Tvis and the MC. Chicks were anaesthetised (0.12ml equithesin, i.p.) and a recording assembly was fitted to the skull, enabling the introduction of tungsten microelectrodes to the IMM, two in each hemisphere (2). The next day, after recovery from anaesthetic, the electrodes were advanced until spontaneous spikes were detected. Each chick was placed in a running wheel and recordings were made during five Tests of neuronal activity (2), though we consider here only T1 (-0.75h) before the start of training, and T5 (25h) after training (times are the mid-point of ~1h tests). Experiments were terminated after the 5th test. The activities of individual neurons (1-12 per electrode) were sorted (2) from the spikes captured at each electrode. Neurons were tested for significant responses (paired t-test, $P<0.05$) during serial 4s presentations (15-20) of the Tvis, the MC, and the TC (Tvis and MC presented together). Comparisons between classes of responsive neurons were made using binary logistic regression. Recordings were made from 230 neurons at T1, and 251 neurons at T5.

The percentage of neurons responding to the TC declined across Tests ($P<0.01$) from T1 (60.4%) to T5 (52.0%). However, by separating those TC-responsive neurons which also responded to the Tvis (TC+Tvis neurons) from those unresponsive to the Tvis (TC-Tvis neurons), we found an increase in TC+Tvis neurons (9.1% to 27.2%, $P<0.001$) similar to that reported previously for Tvis-responsive neurons (2). The decline in TC-responsive neurons is accounted for by a reduction in TC-Tvis neurons (51.3% to 24.8%, $P<0.001$). Most of the TC-Tvis neurons (75.4% at T1, declining to 50.0% at T5, $P<0.001$) were also responsive separately to the MC. In seven untrained chicks 59.2% (142/240) responded to the MC at T1, whereas 31.9% (51/160) did so at T5 ($P<0.001$).

These findings suggest that neuronal changes in the IMM associated with imprinting involve a decrimental process that is largely related to the auditory component of the training compound, and an incremental process related to its visual component.

Horn G (2004). Nat Rev Neurosci 5, 108-120.

Horn G et al. (2001). Proc Natl Acad Sci USA 98, 5282-7.

Supported by BBSRC.

Where applicable, the authors confirm that the experiments described here conform with The Physiological Society ethical requirements.

C18

A study of ankle proprioception using compensatory tracking

M. Lakie[1], T.M. Osborne[1], R.F. Reynolds[1] and I. Loram[2]

[1]School of Sport and Exercise Sciences, Birmingham, Birmingham, UK and [2]Institute of Research into Movement, Manchester Metropolitan, Manchester, UK

In compensatory tracking a subject is required to realign a target which is moved by the experimenter. Unlike pursuit tracking, where the target and the subject's response are separately displayed, the subject experiences only the combined effect of disturbance and correction – steering a boat buffeted by sidewinds is a simple example. The ability to continuously attempt to correct for an offset in this way is not unique to the visual system, for example in nulling disturbances to posture in order to maintain an upright stance corrective responses may be informed by vestibular or proprioceptive senses as well as vision. Despite this, little work appears to have been carried out on compensatory tracking using non-visual senses.

With ethical permission, nine subjects were positioned in a normal standing position while strapped to a backboard. Their feet rested on a footplate which was subjected to computer controlled antero-posterior perturbations with a size and frequency like exaggerated standing sway. The subject was supplied with a joystick which also controlled footplate angle. After appropriate practice the subjects were instructed to attempt to correct for the computer disturbances using only the information from their ankles, so that as far as possible ankle movement was minimized. Four trials were conducted with the intended position of the foot horizontal and four with the intended position 2 degrees of dorsiflexion. For comparison four trials were

conducted with visual information only. In two of these the visual information was by foveation of a fiducial marker, in the other two a looming target provided more "ecological" information akin to visual flow in standing.

All subjects were generally poor compensators. The worst performance was using proprioception with feet horizontal. The best was with explicit visual information. Increased dorsiflexion appeared to be better than feet horizontal. Proprioceptive tracking and "ecological" visual tracking were intermediate (Fig1). The mean delays in the subjects' responses were calculated by cross-correlation. Regression analysis showed that the subjects with the longest delays tended to be the poorest compensators. We conclude that delay and insensitivity to very slow perturbations (drift) combine to severely impair effective compensation.

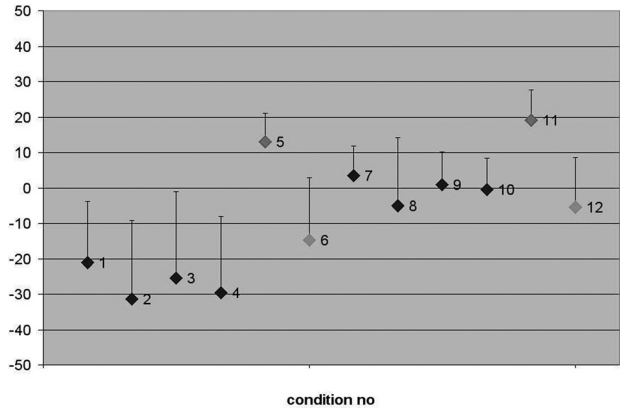

Subjects' effectiveness in sway reduction in different compensatory tracking conditions. A positive percentage denotes a reduction in movement size – ie effective compensation. 100% would be perfect (+95% confidence limit is shown). Subjects were generally very poor compensators. Conditions are: (1 to 4) Proprioceptive tracking feet horizontal, (7 to 10) Proprioceptive tracking feet 2 deg dorsiflexed, (5 & 11) explicit visual feedback, (6 & 12) "ecological" visual feedback The 12 trials were randomized but the figure indicates the order in which each trial was performed by the subject – eg 8 was after 7 and 5 was after 4 etc. Explicit vision (5 & 11) is significantly better than (1 to 4), p=0.006 and (6&12), p=0.034 but not (7 to10), p=0.052. Conditions (7-10) appeared better than conditions (1-4) but this was not significant (p=0.132)

T.O is supported by EPSRC.

Where applicable, the authors confirm that the experiments described here conform with The Physiological Society ethical requirements.

C19

The effect of actual and expected light touch contact on the response to galvanic vestibular stimulation

C.J. Osler, M. Lakie and R.F. Reynolds

School of Sport and Exercise Sciences, University of Birmingham, Birmingham, UK

Information from the somatosensory system modulates the postural response to a vestibular-evoked perturbation (galvanic vestibular stimulation, GVS; for review see Fitzpatrick and Day, 2004). A previous study investigating the effect of lightly touching a fixed support reported a reduced muscular response to GVS compared to normal standing (Britton et al., 1993). Here, we further investigate this modulation. Firstly, we studied the effect of small quantified changes in the light touch contact force on the evoked whole body response. Secondly, we investigated if merely an expected change in light touch information could modulate the response to GVS. In the first experiment subjects (n=9) were instructed to stand in the required start position (with vision occluded and their back in contact with a foam pad) while GVS (1 mA for 3 seconds) was applied. Five conditions each studying different target contact forces were used (0N, 0.5N, 1N, 3N and 6N). Results showed the GVS-evoked lateral body displacement was strongly affected by condition ($F_{4,32} = 30.48$, $p<0.001$; repeated measures ANOVA); it was significantly attenuated in all light contact conditions compared to normal standing (all $p<0.05$; pairwise comparisons with Bonferroni adjustment), including the lowest contact force condition (mean ± S.D.; 0.52 ± 0.13N) where the mechanical advantage provided was minimal. This suggests the attenuated postural response to GVS with light touch contact is partly due to additional cutaneous sensory information and not merely mechanical stabilisation. In light contact conditions the response size was then scaled according to the measured contact force ($r^2 = 0.35$, $p<0.001$; linear regression). In the second experiment the light touch information available to the subjects could be withdrawn by way of a servo motor. From the same start position the subjects (n=10) self-triggered GVS (2 mA for 0.6 seconds). Subjects expected a simultaneous removal of light touch information in some trials (expected no contact condition) and no such removal in the remainder (expected contact condition). However, in 20% of the expected no contact trials the removal of light touch information did not actually occur (unexpected contact condition). Results showed the postural response was again significantly affected by condition ($F_{2,18} = 17.28$, $p<0.001$; repeated measures ANOVA). However, in contact conditions results showed that GVS evoked a sway response that was not affected by whether the sensory information attained from light touch contact was expected or unexpected ($p = 1.00$; pairwise comparison with Bonferroni adjustment). This suggests that merely an expected change cannot modulate the evoked response in the same way as an actual change in light contact information.

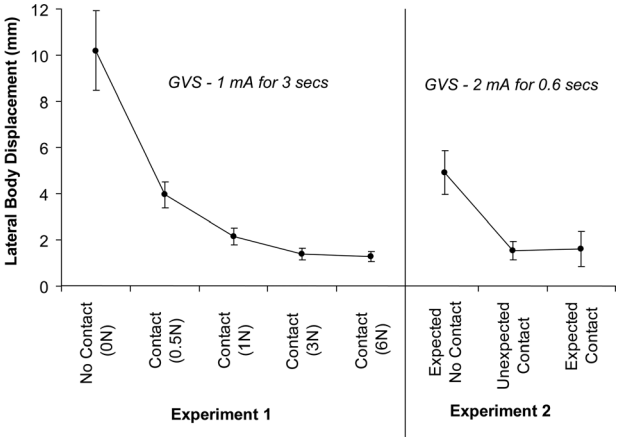

Mean (± S.E.M) peak lateral body displacement in the direction of the anodal ear.

Britton TC *et al.* (1993). *Experimental Brain Research* **94**, 143-151.

Fitzpatrick RC & Day BL (2004). *Journal of Applied Physiology* **96**, 2301-2316.

Where applicable, the authors confirm that the experiments described here conform with The Physiological Society ethical requirements.

C20

An accessible "Integration Surface" in a jellyfish nervous system

R.W. Meech[1] and G.O. Mackie[2]

[1]Department of Physiology & Pharmacology, University of Bristol, Bristol, UK and [2]Biology, University of Victoria, Victoria, BC, Canada

Jellyfish nervous systems, among the earliest to evolve, and among the simplest in structure, integrate sensory signals from vibration, taste, gravity and photo-receptors with an on-going pacemaker activity that drives swimming. Integration of visual stimuli by Cubomedusae (box jellyfish) allows them to avoid obstacles while statocysts removal produces directionless swimming in many jellyfish forms. Other aspects of swimming modulated by sensory input include swim strength and swim frequency. The data reported are from a small hydrozoan jellyfish, *Aglantha digitale*, which escapes from predators by jet propulsion via contractions in its bell-shaped body wall (Donaldson, *et al*., 1980).

Taste receptors affect swim frequency. When feeding, Aglantha stops swimming, perhaps because the high velocity water flow generated would otherwise detach captured prey from its mouth and tentacles (Mackie *et al*., 2003). The inhibitory signal which is initiated following manipulation of the prey by the mouth of the jellyfish is conducted to pacemaker cells distributed in a ring around the base of the animal (Mackie & Meech, 2008).

Vibration sensors affect swim strength. Hair cell-like structures at the base of *Aglantha* (Arkett *et al*., 1988) sense vibrations produced by predators and trigger strong "escape" swims. The overall form of the contraction of the body wall associated with escape swimming differs from that during a normal "slow" swim. During escape swims the contraction is uniform while during slow swimming the contraction is confined to the upper half of the bell and is strongest near the eight radial giant motor axons that innervate the body wall.

A combination of intracellular and "loose patch" (Roberts & Almers, 1992) recordings have revealed the different integrative processes that produce such varied swimming outcomes. Following a mechanical stimulus at the base of *Aglantha* a depolarizing post-synaptic potential (psp) activates voltage-gated sodium channels in the motor axon. The overshooting action potential elicited initiates widespread contraction in the sheet of electrically coupled muscle cells in the body wall. The low amplitude psp arising from the pacemaker system activates a low-threshold, low amplitude calcium spike based on activation of "T"-type calcium channels. Unlike the psp the calcium spike is propagated regeneratively and becomes large enough to activate low threshold channels in the muscle membrane. The associated contraction is weaker and more restricted.

Conclusion: Complex behaviour in jellyfish arises from an easily accessible "Integration Surface" where propagating and "passive" electrical signals interact in a way that depends on the specific voltage-driven properties of specialized ion channels.

Arkett, S.A., Mackie, G.O. & Meech, R.W. (1998). Hair Cell Mechanoreception in the Jellyfish *Aglantha digitale*. J. Exp. Biol. 135, 329-342.

Donaldson, S., Mackie, G.O. & Roberts, A. (1980). Preliminary observations on escape swimming and giant neurons in *Aglantha digitale* (Hydromedusae: Trachylina). Can. J. Zool. 58, 549—552.

Mackie, G.O., Marx, R.M. & Meech, R.W. (2003). Central circuitry in the jellyfish *Aglantha digitale* IV. Pathways coordinating feeding behaviour. J. Exp. Biol. 206, 2487-2505.

Mackie, G.O. & Meech, R.W. (2008). Nerves in the endodermal canals of hydromedusae and their role in swimming inhibition. Invert Neurosci. 8, 199-209.

Roberts, W.M. & Almers, W.(1992). Patch voltage clamping with low-resistance seals: loose patch clamp. Methods Enzymol. 207, 155-176.

We thank the director and staff of Friday Habor Laboratory, University of Washington, USA, for their help and for making research facilities available to us.

Where applicable, the authors confirm that the experiments described here conform with The Physiological Society ethical requirements.

PC01

Boxing head-guards do not prevent Cerebral Trauma

M.R. Graham[1,2], T. Myers[1], N.E. Thomas[4], B. Davies[2], S.M. Cooper[5], P.J. Evans[3] and J.S. Baker[6]

[1]PESS, Newman University College, Birmingham, UK, [2]HESAS, Glamorgan University, Cardiff, UK, [3]Department of Endocrinology, Royal Gwent Hospital, Newport, UK, [4]Centre for Child Research, Swansea University, Swansea, UK, [5]Cardiff School of Sport, University of Wales Institute Cardiff, Cardiff, UK and [6]Health & Exercise Science Research Unit, University of the West of Scotland, Hamilton, Scotland, UK

Mild brain injuries (MBIs) in boxing are a major public concern due to the risk of accumulative effects. The severity of traumatic brain injury is associated with the early post-traumatic release of protein S-100B and neurone specific enolase (NSE). Their early kinetics after traumatic brain injury reflect intracranial pathology as demonstrated in cranial computerised tomography (CT) and they have become an extremely sensitive prognostic marker associated with neuropsychological outcome even in minor head injury (Herrmann et al., 2001).

Boxing bouts are often stopped because of facial cuts, which have little impact on neuro-cognitive performance, but look horrific because of the sight of blood. However, bouts are allowed to continue after serious knockdowns, following blows to the head. There is evidence that markers for cerebro-spinal fluid levels of neuronal and axonal injury are still present, three months following a bout of boxing (Zetterberg et al., 2006) and it is often impossible to keep track of the majority of subjects to establish when serum levels return to baseline.

Serum cortisol, is known to be elevated following head trauma (King et al., 1970) and prolonged hypercortisolaemia can lead to unipolar depression and dopaminergic, noradrenergic and thyroid dysfunction (Duval et al., 2006).

The aim of this study was to analyse whether punches to the head (PTH), sustained during a single amateur boxing bout of five, two minute rounds, would result in cerebral damage.

The boxers were divided into two groups, retrospectively following the boxing contest. Following this analysis, male subjects (n=16) were assigned into:

Punches to the head group (PTH), (n=8, mean ± SD, age: 17.6 ± 5.3 years; height: 168.4 ± 13, cm; weight: 65.4 ± 20.3, kg; Punches to the body group (PTB), (n=8, mean ± SD, age: 19.1 ± 3.2 years; height: 169.6 ± 7.5, cm; weight: 68.5 ± 15, kg). The PTH group received punches to the head and body, while group PTB received only punches to the body. Blood samples were taken pre- and immediately post combat for analysis of S-100B, neurone specific enolase (NSE), cortisol, creatine kinase (CK) and troponin.

Significant increases ($P<0.05$) in serum concentrations of S-100B (0.35 ± 0.61 vs 0.54 ± 0.73, μg.L-1), NSE (19.7 ± 14 vs 31.1 ± 26.6, ng.ml-1) and cortisol (372.9 ± 201.5 vs 755.8 ± 93, nmol.L-1) were encountered post combat in the PTH group and CK in both groups (PTH: 207 ± 107 vs 244 ± 118, U/L; PTB: 150 ± 43 vs 195 ± 63, U/L). There were no elevated levels of troponin.

PTH in amateur boxing are sufficient enough to cause biochemically discernible damage to brain tissue. There is a direct correlation between elevated serum cortisol levels and dysthymia. The consequences of MBI may appear simple, nonetheless, transitory post-concussive syndrome can often progress to psychological chronic post traumatic stress disorder (Vanderploeg et al., 2009).

Duval F et al. (2006). Psychoneuroendocrinology 31, 876-888.

Herrmann M et al. (2001). J Neurol Neurosurg Psychiatry 70, 95-100.

King LR et al. (1970). Ann Surg 172, 975-984.

Zetterberg H et al. (2006). Arch Neurol 63, 1277-1280.

Vanderploeg et al. (2009). Arch Phys Med Rehabil 90, 1084-1093.

Morriston Hosp., Swansea

Where applicable, the authors confirm that the experiments described here conform with The Physiological Society ethical requirements.

PC02

Long-term actions of BDNF on inhibitory synaptic transmission in identified neurons of the rat *Substantia gelatinosa*

P.A. Smith[1] and V.B. Lu[2]

[1]Department of Pharmacology, University of Alberta, Edmonton, AB, Canada and [2]Laboratory of Neuropharmacology, NIH/NIAAA, Rockville, MD, USA

Peripheral nerve injury promotes the release of brain derived neurotrophic factor (BDNF) from spinal microglial cells and primary afferent terminals (Coull *et al.,* 2005). This induces a series of changes in the properties of neurons in the dorsal horn that lead to the 'central sensitization' that underlies neuropathic pain (Merighi *et al.,*2008). Several lines of evidence implicate the impairment of GABAergic and/or glycinergic inhibition in this process (Coull *et al.,* 2005). To test this possibility further, we used a defined medium organotypic culture of rat spinal cord to examine changes in inhibitory synaptic transmission in *substantia gelatinosa* following 6d exposure to BDNF (200ng/ml). This duration of exposure seeks to mimic the prolonged increase in dorsal horn BDNF levels that accompany peripheral nerve injury. We used morphological and electrophysiological criteria as well as glutamic acid decarboxylase (GAD) immunohistochemistry to distinguish putative inhibitory

neurons from putative excitatory neurons. Spontaneous IPSCs (sIPSCs) were recorded by means of whole-cell recording. BDNF exerted both pre- and postsynaptic effects on inhibitory synaptic transmission that were selective for neuron type. In putative excitatory 'delay' firing neurons, it increased sIPSC amplitude from 49.3±1.5 to 64.8±1.7pA (P<0.001), interevent interval (IEI) was reduced from 1089.9±34.7 to 776.4±18.3ms (P<0.01). In 'tonic' firing, putative inhibitory neurons, BDNF had little effect on sIPSC amplitude (67.6±1.9pA in control, 67.1±2.6pA in BDNF, ns). It did however increase IEI from 780.1±16.1 to 1174.7±37.8ms (P<0.001). Increased inhibitory drive to excitatory neurons and decreased inhibitory drive to inhibitory neurons seem inconsistent with our previous observation that BDNF increases overall dorsal horn excitability(Lu *et al.,* 2007;Lu *et al.,* 2009). Our results also contrast with published findings in Lamina I where impairment of inhibition may play a major role in central sensitization and/or the actions of BDNF (Coull *et al.,* 2005). It is therefore suggested that central sensitization at the level of the *substantia gelatinosa* may reflect previously documented BDNF-induced increases in excitatory transmission (Lu *et al.,* 2007;Lu *et al.,* 2009)rather than decreases in inhibitory transmission.

Coull JA *et al* (2005). *Nature* **438**, 1017-1021.

Lu VB *et al* (2007). *J Physiol.,* **584**, 543-563.

Lu VB *et al* (2009. *J Physiol.,* **587**, 1013-1032.

Merighi A *et al* (2008). *Prog. Neurobiol.* **85**, 297-317.

Supported by the Canadian Institutes of Health Research (CIHR; Funding reference # 81089).

Where applicable, the authors confirm that the experiments described here conform with The Physiological Society ethical requirements.

PC03

Craniocentric vertical torque responses to vestibular stimulation

R.F. Reynolds

School of Sports and Exercise Sciences, University of Birmingham, Birmingham, UK

Electrical stimulation of the vestibular nerve causes walking subjects to turn left or right, depending upon head pitch and stimulus polarity (1). Such responses require the stance leg to generate torque around a vertical axis. Whether this also occurs with both feet on the ground is open to question. Here I determine the effect of vestibular stimulation upon vertical torque (free Z moments) when standing quietly, and see whether the response is modulated by head position.

Square-wave current stimuli (2mA, 3s) were applied to the mastoid processes in subjects standing on a force plate with eyes closed and feet together. With the head facing 60 degrees down and the anode electrode behind the right ear, small but significant torque oscillations were observed. These occurred with a latency of 100ms, reaching a peak of 0.05 Nm at 190ms, lasting around 1s. This response was accompanied by clockwise trunk rotation (0.3 deg/s peak). Reversing stimulus polarity caused an equal response in the opposite direction. With the head facing forwards the stimulus had no significant effect upon torque.

Stochastic Vestibular Stimulation (SVS; 0-5Hz, 1.5mA RMS) was used to investigate the effect of head position in greater detail, allowing the response to be characterised in time and frequency using cross-correlations and cross-spectra, respectively (2). The cross-correlation was smoothly modulated by head pitch, being maximal with the head up and down, reaching a minimum with the head approximately level (-8 deg; see Fig 1). However, coherence analysis revealed two distinct frequency responses at 3 and 7 Hz. The former was heavily modulated by head pitch, whereas the latter was not.

These data provide evidence of craniocentric vertical torque responses to vestibular stimulation when standing. The observed modulation of the response with head pitch is consistent with the CNS interpreting the stimulus as head rotation around a naso-occipital axis, due to canal activation (3). Previous research also shows the presence of an additional shorter latency response to vestibular stimulation due to otolith activation (4), resulting in lateral force responses. In the current experiment, mechanical coupling between lateral force and torque would explain the presence of the high frequency torque response unaffected by head position. In support of this, cross correlations between force and torque revealed significant peaks at positive lags. Hence, low frequency stimulation (0-5Hz) is best suited to assessing the influence of neck pitch upon the vestibular-torque response, since it primarily activates the canal response.

The technique described here constitutes a new experimental tool with which to assess neck proprioception in the pitch axis. This could be used to quantify alterations in neck sensation caused by pathology or sensory illusions (5).

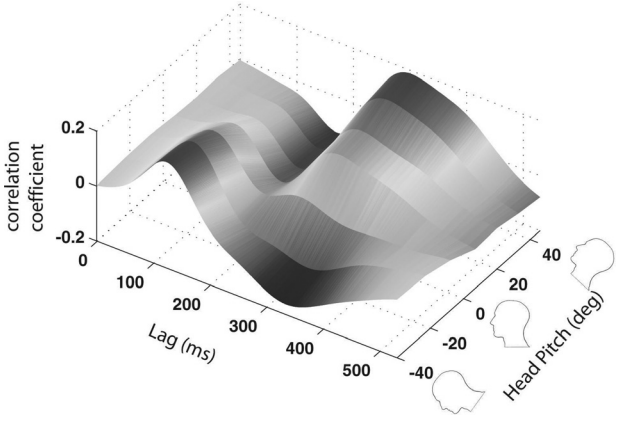

Figure 1. Modulation of SVS-Torque Cross Correlation by Head Pitch

Randomly varying current (SVS) was applied between the mastoid processes continuously for 80s. Vertical torque was measured concurrently.

Subjects were asked to adopt a specific head pitch during each trial (+/- 45 deg). Head pitch was measured as the angle of Reid's plane versus horizontal. The relationship between SVS and torque was then assessed by cross correlation.

Fitzpatrick RC, Butler JE, Day BL. Resolving head rotation for human bipedalism. Curr Biol 2006;16:1509-1514.

Dakin CJ, Son GM, Inglis JT, Blouin JS. Frequency response of human vestibular reflexes characterized by stochastic stimuli. J Physiol 2007;583:1117-1127.

Day BL, Fitzpatrick RC. Virtual head rotation reveals a process of route reconstruction from human vestibular signals. J Physiol 2005;567:591-597.

Cathers I, Day BL, Fitzpatrick RC. Otolith and canal reflexes in human standing. J Physiol 2005;563:229-234.

Gurfinkel VS, Popov KE, Smetanin BN, Shlykov VI. Changes in the direction of vestibulomotor responses in the process of adaptation to prolonged static head turning in man. Neirofiziologiia 1989;21:210-217.

Where applicable, the authors confirm that the experiments described here conform with The Physiological Society ethical requirements.

PC04

Maturation of excitatory synaptic transmission occurs more slowly in mouse primary visual cortex than in barrel cortex

C.E. Cheetham and K.D. Fox

School of Biosciences, Cardiff University, Cardiff, UK

The development and plasticity of cortical circuits has been widely studied in both whisker barrel cortex (BC) and primary visual cortex (VC)(1). During repetitive stimulation, postsynaptic responses undergo short-term synaptic plasticity. Synapses generally switch from strong depression to weaker depression or facilitation between the second and fifth postnatal weeks (2). Although the timing of developmental critical periods differs between BC and VC (1), a comparison of the development of synaptic properties in BC and VC has not been made. We made whole cell recordings of layer 2/3 (L2/3) pyramidal neurons at 35 – 37°C in acute brain slices from postnatal day (P)12–P138 C57BL/6 mice, and applied short stimulus trains to presynaptic axons. Statistics were calculated from paired-pulse ratios (PPR) at 20 Hz (mean±S.E.M.) using t-tests unless stated. For horizontal connections within L2/3, PPR increased dramatically between P12 and P28 in both BC (0.96±0.08 to 1.13±0.03) and VC (0.89±0.06 to 1.21±0.05; P<0.001 for age, P=0.86 for area, two-way ANOVA). In the L4 to L2/3 pathway, there was also a marked increase in PPR in BC between P12 and P28 (0.90±0.09 to 1.11±0.08, P=0.045), which was blocked by total bilateral whisker deprivation (0.94±0.04, P=0.74 vs P12). In contrast, VC synapses exhibited similar short-term plasticity at P12 and P28 (0.93±0.05 to 0.96±0.05, P=0.73), but underwent a significant increase in PPR between P28 and P43 (to 1.10±0.04, P=0.029). No further changes were seen in either area up to P138 (P=0.86, one-way ANOVA), indicating that synaptic maturation is complete by P28 in BC, and P43 in VC. Short-term synaptic dynamics are thought to reflect presynaptic release probability: lower release probability results in greater facilitation (3). Therefore, we compared release probability in the L4 to L2/3 pathway at P28, when BC has matured but VC has not, by measuring the rate of use-dependent blockade of NMDARs (N-methyl-D-aspartate receptors) by MK-801. Use-dependent blockade occurred more slowly in BC than in VC (% block after 100 trials: VC 17±4%, BC 31±5%, P<0.001 for cortical area and trial number, two-way ANOVA), indicating a lower release probability in BC than VC. Our data show that synapses in primary sensory cortex continue to mature until six weeks of age, and highlight the interplay between development and plasticity. Maturation involves a reduction in presynaptic release probability and concomitant increase in short-term facilitation. In the L4 to L2/3 pathway, maturation occurs two weeks later in VC than in BC, in keeping with the relative timing of developmental critical periods in the two areas. Greater short-term facilitation at mature synapses will enhance the temporal fidelity of signal processing at higher stimulus frequencies.

Fox K & Wong RO (2005). *Neuron* **48**, 465-77.

Feldmeyer D & Radnikow G (2009). *J Physiol*, **587** 1889-96.

Zucker RS & Regehr WG (2002). *Annu Rev Physiol* **64**, 355-405.

Funded by the NIMH and MRC

Where applicable, the authors confirm that the experiments described here conform with The Physiological Society ethical requirements.

PC05

The role of GluR1 in experience dependent depression in the visual cortex

A. Ranson, K.D. Fox and F. Sengpiel

School of Biosciences, Cardiff University, Cardiff, UK

Primary sensory cortex is capable of adapting to altered sensory input, a process termed experience dependent plasticity. One form of adaptation is depression at the synaptic level of an input that no longer provides coherent sensory information. In a recent study we found complementary in vivo and in vitro evidence that this type of depression (as induced by whisker removal) in L2/3 of the mouse somatosensory cortex (S1) is dependent upon the presence of the GluR1 AMPA-R subunit (Wright, Glazewski et al., 2008). We have now examined whether an analogous process of depression in the visual cortex (V1) may also be GluR1 dependent. Suturing the eyelid of a mouse (monocular deprivation, MD) for 3d at the height of the critical period (P26-P29) has been reported to cause a robust 30-50% depression of the layer 2/3 V1 response to visual stimulation after eye reopening (Cang et al., 2005). This depression occurs both in the binocular region of V1 which receives input from both eyes, and the monocular region which only receives contralateral eye input.

Using intrinsic signal imaging we compared the cortical responses of anesthetised mice following either normal visual experience or three days of monocular visual experience at the height of the critical period. Eye lid suture was conducted under 2% isoflurane anaesthetic administered in oxygen, while imaging was carried out under 0.8-1% isoflurane administered in oxygen and supplemented with a single intramuscular injection of 25μg chlorprothixene.

The baseline V1 responses to visual stimulation in both the binocular and monocular areas were attenuated in GluR1$^{-/-}$ mice by around 40% (for example in the binocular area, WT mean ± SEM: 27.8x10^{-5} ± 3.5x10^{-5}, n=6; GluR1$^{-/-}$ mean ± SEM: 16.4x10^{-5} ± 1.7x10^{-5}, n=10, t-test: p<0.01). In binocular cortex, 3d of MD resulted in a percentage depression of closed eye responses relative to genotype baseline which did not differ significantly

between genotypes (WT mean depression ± SEM: 49% ± 6%, n=5, t-test: p<0.01; GluR1$^{-/-}$ mean depression ± SEM: 41% ± 4%, n=9, t-test: p<0.05). In contrast, in the monocular region of V1, 3d of MD resulted in a percentage response depression in WT mice, while no significant depression was observed in GluR1$^{-/-}$ mice (WT mean depression ± SEM: 37% ± 4%, n=9, t-test: p<0.05; GluR1$^{-/-}$ mean depression ± SEM: 7% ± 1%).

Our findings suggest that depression mechanisms operate differently in monocular and binocular regions of visual cortex and that only the former is GluR1 dependent. This suggests that GluR1 may be more important for homosynaptic depression mechanisms not requiring direct competition for depression to occur and that other mechanisms occur in binocular cortex.

Cang J, Kalatsky VA, Löwel S & Stryker MP. (2005). Optical imaging of the intrinsic signal as a measure of cortical plasticity in the mouse. Vis Neurosci 22, 685-691.

Wright N, Glazewski S, Hardingham N, Phillips K, Pervolaraki E & Fox K. (2008). Laminar analysis of the role of GluR1 in experience-dependent and synaptic depression in barrel cortex. Nat Neurosci 11, 1140-1142.

MRC Grant G0500186 to FS, MRC Grant G0200413 to KF

Where applicable, the authors confirm that the experiments described here conform with The Physiological Society ethical requirements.

PC07

Low frequency stimulation induces a group II metabotropic glutamate receptor dependent LTD in the cortical input to the lateral amygdala

S.J. Lucas, G.L. Collingridge, D. Lodge and Z.A. Bortolotto

MRC Centre for Synaptic Plasticity, Department of Anatomy, University of Bristol, Bristol, UK

Group II metabotropic glutamate receptors (mGluRs) are G-protein coupled receptors, which are negatively linked to adenylyl cyclase. There are two subtypes of group II mGluRs; mGluR2 and mGluR3, which are located perisynaptically in many brain regions and are thought to act as autoreceptors of glutamatergic synaptic transmission. The activation of group II metabotropic glutamate receptors has been shown to cause a lasting depression of synaptic transmission both within the basolateral amygdala complex and in thalamic afferents to the lateral amygdala (Heinbockel and Pape, 2000; Lin et al., 2000). It has been suggested that low frequency stimulation (LFS) induced long-term depression (LTD) within the basolateral amygdala complex may involve group II mGluRs (Wang & Gean, 1999; Kaschel et al., 2004). However the role of group II mGluRs in modulating transmission and in particular plasticity within the cortical input to the lateral amygdala is not clear. We have therefore investigated the role of group II mGluRs in this cortical input to the lateral amygdala.
Experiments were performed on acute coronal amygdala slices from adult male CD-1 mice. Whole-cell patch-clamp recordings were made from pyramidal-type cells in the lateral amygdala while stimulating the external capsule, which contains the cortical input to the lateral amygdala.

We show that the pharmacological activation of group II mGluRs with the selective agonist, DCG-IV, induces a dose-dependent long-term depression of synaptic transmission; 1 μM DCG-IV results in a persisting depression of 46 ± 10 % (± S.E.) at 60 min post application (n=8). The DCG-IV induced depression is associated with a transient increase in paired pulse facilitation (68 ± 15 %, n=6), suggesting that the initial depression may involve a presynaptic mechanism, while the long-term depression may involve a postsynaptic mechanism. In the cortical input to the lateral amygdala a low frequency stimulation protocol (900 pulses at 1 Hz, holding cells at -70mV) is found to induce LTD (39 ± 6 % at 40 min post LFS, n=10). This LFS-LTD is dependent upon the activation of group II mGluRs, as it can be blocked by LY341495, a group II mGluR selective antagonist at 300 nM. The NMDA antagonist, D-AP-5 (50 μM) also blocks this LTD, suggesting that NMDA receptor activation is also involved in mediating this LFS-LTD.

Heinbockel & Pape (2000). The Journal of Neuroscience 20, 1-5.

Kaschel et al. (2004) Synapse 53, 141-150

Lin et al. (2000). The Journal of Neuroscience 20, 9017-9024.

Wang & Gean (1999) The Journal of Neuroscience 19, 10656-10663

Supported by MRC and Eli Lilly and Co. Ltd.

Where applicable, the authors confirm that the experiments described here conform with The Physiological Society ethical requirements.

PC08

Characterisation of AMPAR trafficking at associational commissural synapses in the CA3 region of the hippocampus following Oxygen Glucose Deprivation

S. Dennis and J. Mellor

MRC Centre for Synaptic Plasticity, Department of Anatomy, University of Bristol, Bristol, UK

The hippocampus is important in learning and memory and is particularly susceptible to delayed cell death following stroke. Within the hippocampus, there is evidence that CA1 pyramidal neurones are more susceptible to ischaemic damage than cells in the CA3 region, but exact reasons why remain unknown. One major excitatory postsynaptic receptors within the hippocampus is the AMPA receptor (AMPAR). The plasticity of AMPA receptors in postsynaptic hippocampal slices following oxygen glucose deprivation (OGD), conditions believed to replicate those found in ischaemia, has previously been demonstrated in CA1 pyramidal neurones where synaptic AMPAR subunit switching occurs following OGD [1]. Here we show a selective substantial decrease in AMPAR excitatory postsynaptic currents (EPSCs) following OGD at associational-commissural (AC) synapses in the CA3 area but not at CA1 Schaffer collateral synapses.<p>
Experiments were performed using hippocampal slices taken from postnatal day (P) 13-15 rats. Whole-cell patch clamp recordings and extracellular field potential recordings were made in the presence of the NMDAR antagonist Ly-689,560 (5μM) and GABAA receptor antagonist picrotoxin (100μM) to investigate changes in AMPAR trafficking at the membrane in

response to 15 minutes OGD (O2 and glucose replaced with N2 and sucrose respectively).<P>
OGD resulted in a substantial and long-lasting loss of AMPAR-mediated EPSCs on CA3 pyramidal neurones (86±14%, n=7). The fibre volley amplitude was transiently depressed during OGD, followed by a full recovery within 30 minutes (107±18%, n=7) suggesting that the decrease in AMPAR EPSC amplitude was not due to a loss of presynaptic firing. Further evidence for a postsynaptic AMPAR loss was demonstrated by measuring responses to exogenous glutamate (10mM) application to evoke AMPAR-mediated responses. Responses to exogenous glutamate were also depressed following OGD (4±2% n=9). The effect was specific to AMPARs and localised within the CA3 region as NMDAR-mediated EPSCs and Schaffer collateral synaptic responses in CA1 both recovered following OGD (63±10% n=11 and 77±24%, n=4). The addition of 2mM Kynurenate during OGD failed to recover the AMPAR EPSC (1±2%, n=8), suggesting that the loss of the AMPAR EPSC is not dependent on AMPAR activation. However, removal of Ca2+ from the external solution during OGD (71±7%, n=10), or the addition of 50μM BAPTA to the intracellular solution (78±10%, n=10), was able to prevent the loss of AMPAR EPSCs normally observed. <P> We conclude that there is a selective decrease of postsynaptic AMPAR EPSC at AC synapses within the CA3 region of the hippocampus following OGD that is not mediated by NMDAR or AMPAR activation but requires a rise in intracellular Ca2+.

Dixon, R.M., J.R. Mellor, and J.G. Hanley, PICK1-mediated Glutamate Receptor Subunit 2 (GluR2) Trafficking Contributes to Cell Death in Oxygen/Glucose-deprived Hippocampal Neurons. Journal of Biological Chemistry, 2009. 284(21): p. 14230-14235.

Where applicable, the authors confirm that the experiments described here conform with The Physiological Society ethical requirements.

PC09

Development of human infant pain behaviour: Nociceptive flexion withdrawal reflex EMG activity and facial motor responses in preterm and term infants

L. Cornelissen[1], R. Slater[1], S. Boyd[2] and M. Fitzgerald[1]

[1]Department of Neuroscience, Physiology and Pharmacology, University College London, London, UK and [2]Clinical Neurophysiology, Great Ormond Street Hospital for Children, London, UK

INTRODUCTION: Premature infants in intensive-care are exposed to multiple painful procedures as part of necessary clinical care. Nociceptive flexion reflex withdrawal and facial motor activity are used as measures of spinal nociceptive processing and are important components of pain behaviour. Here we compare the pattern of nociceptive flexion reflex activity in preterm and term infants following clinically required heel lances. For each infant we also compare the flexion reflex with facial motor behaviour. METHOD: The noxious stimulus was a time-locked clinical heel lance. A non-noxious sham was applied by rotating a heel lancet so that the blade did not contact the heel. Flexion withdrawal reflex activity was recorded from the ipsilateral biceps femoris using surface EMG in 12 preterm(32–36.9wk postmenstrual age) and 18 term(37–43wk) infants. Activity from the contralateral biceps femoris was recorded on 17 occasions (7 preterm,10 term). The evoked activity was quantified by calculating the root mean square (RMS) of the EMG signal in 250 ms bins. Facial motor activity was simultaneously video-recorded and infants were classified according to whether or not they exhibited facial motor behaviour (12 preterm,10 term). RESULTS: Noxious stimulation evoked EMG activity in the ipsilateral biceps femoris in all infants. EMG activity was maintained for at least 1.5s and was significantly greater than the sham in all infants ($p<0.01$, 2-way ANOVA). Preterm and term infants showed different patterns of noxious-evoked EMG activity; preterm infants exhibited a sustained response (mean±sem; RMS_{250ms}post-onset= 28.23±4.31μV, RMS_{1s}post-onset= 26.24±8.04μV); term infants exhibited an initial phase of increased muscle activity and a late phase of reduced but sustained activity(RMS_{250ms}= 50.77±6.64μV, RMS_{1s}= 19.55±3.64μV). The pattern of response in both preterm and term infants was synchronous in the ipsilateral and contralateral leg with no significant differences in the post-onset activity. Flexor EMG activity was always evoked by noxious heel lance whereas changes in facial expression were not observed in 18% (4/22) of infants. CONCLUSION: The pattern of flexor motoneurone activity evoked by a noxious stimulus differs in preterm and term infants. Late-phase reduced activity seen in term infants may reflect the influence of supraspinal inhibitory input. Coincident activation of both muscles in all age groups indicates an immature balance of spinal excitation and inhibition, with focused limb withdrawal occurring at a later age in development. EMG recordings of flexion reflex withdrawal are more sensitive measures of noxious-evoked activity in infants than observed changes in facial behaviour.

This work is supported by the MRC and the British Pain Society.

Where applicable, the authors confirm that the experiments described here conform with The Physiological Society ethical requirements.

PC10

Involvement of PKC in SUMOylation and kainate receptor trafficking

S. Chamberlain and J. Mellor

MRC centre for Synaptic Plasticity, Department of Anatomy, University of Bristol, Bristol, UK

SUMOylation is a post-translation modification whereby a member of the SUMO family is covalently attached to other proteins to modify their function, similar to ubiquitination. SUMOylation, has been found to have many functions, the most studied of which are nuclear-cytosolic transport and transcriptional regulation. However, more recently SUMO was found to be involved in the activity dependent removal of GluK2-containing kainate receptors (KAR) from the plasma membrane (1). PKC has been shown to have a role in both removal (2;3) and insertion of KAR (4;5). In addition, the GluK2 subunit has a predicted PKC phosphorylation site close to the consensus sequence for SUMOylation. We therefore investigated the role

of PKC in SUMO-dependent internalisation of GluK2-containing KAR using whole cell patch clamp electrophysiology in CA3 pyramidal neurons in transverse hippocampal slices from P14 Wistar rats. All data are given as a percentage of the initial response and error values stated refer to the standard error of the mean.

In agreement with Martin et al. (2007), inclusion of SUMO-1 in the patch pipette solution decreases the amplitude of KAR-EPSCs to 50.0 ± 4.4% (n=13). In addition, inclusion of SENP-1, an enzyme responsible for de-SUMOylation, increases amplitude to 134.9 ± 7.2% (n=7), thought to be due to reinsertion of receptors that are no longer SUMOylated. However, application of phorbol 12-myristate 13-acetate (PMA; 1 μM), a PKC activator, increased KAR-EPSC amplitude to 140.0 ± 11.0% (n=7; P<0.05). Whilst application of a PKC inhibitor, chelerythrine (5 μM) decreased KAR-EPSC amplitude to 73.4 ± 8.3% (n=7; P<0.05). These data imply that phosphorylation of PKC does not lead to SUMOylation.

Conversely, preincubation with PMA (1 μM) for 15 minutes leads to an increase in the SUMO-1 dependent rundown of KAR-mediated EPSCs (55.6 ± 7.7% vs 26.1 ± 5.2%; n=8; P<0.05). Also, incubation with chelerythrine occludes the SUMO-1 dependent rundown (93.56 ± 8.3%, n=8). We propose that phosphorylation of GluK2 leads to insertion or stabilisation of GluK2-containing receptors in the membrane, increasing the number of receptors in the membrane that may subsequently be SUMOylated. When receptor recycling is blocked using chelerythrine there is a slow rundown in the number of synaptic receptors and therefore less receptors to be SUMOylated. In support of this, preincubation with PMA has no effect on the run-up in KAR-EPSC amplitude caused by SENP-1 (138.15 ± 6.7% vs. 139.34 ± 9.5%), but blocking PKC also occludes the SENP-1 run-up (94.1 ± 7.4%).

Taken together, these data suggest that PKC is involved in the trafficking of KAR at mossy fibre synapses in CA3. Rather than leading directly to SUMOylation, phosphorylation of GluK2 by PKC may increase or stabilise receptors at the synapse, and these receptors are likely to be from the same pool of KAR that can be SUMOylated.

Martin et al. (2007). Nature. 17; 447(7142):321-5.

Rivera et al (2007). EMBO J. 17; 26(20):4359-67.

Selak et al (2009) Neuron. 13; 63(3):357-71.

Hirbec et al (2003) Neuron. 20; 37(4):625-38.

Park et al (2005) Neuron. 5; 49(1):95-106.

Where applicable, the authors confirm that the experiments described here conform with The Physiological Society ethical requirements.

PC11

Experience-dependent regulation of functional maps and protein expression in visual cortex

S. Jaffer[1], V. Vorobyov[1], P.C. Kind[2] and F. Sengpiel[1]

[1]School of Biosciences, Cardiff University, Cardiff, UK and [2]School of Biomedical Sciences, University of Edinburgh, Edinburgh, UK

The primary visual cortex (V1) is a model system for the study of synaptic plasticity. Although some of the receptors associated with ocular dominance (OD) plasticity in cats have been examined, the role of downstream signalling molecules has received scant attention. We therefore examined how glutamate receptor subunits and their downstream signalling molecules and GABA receptor subunits are regulated developmentally and whose expression is dependent on sensory experience.

We assessed the functional architecture of VI using optical imaging of intrinsic signals in anaesthestised cats (1.0-2.5% isoflurane in 60% N2O and 40% O2). We obtained OD and orientation maps from cats reared normally (10 days, 3, 5 12 weeks and 1 year old) or in complete darkness (DR) (3, 5 and 12 weeks old, n=2 or 3 per age group). Animals were euthanised and V1 was removed and homogenised, followed by immunoblotting for quantification of protein expression. We found that visual experience is not required for the establishment of OD and orientation maps, since these were distinct in DR cats at 5 weeks. In contrast, in 12 weeks old DR cats, maps were barely discernible; therefore visual experience is required for their maintenance. Developmentally, the expression of NR2B and SAP-102 declined with age while NR2A, pMAPK and mGluR5 peaked at 5 weeks of age. The expression of NR1, GluR1, GluR2/3, PKC, PKARIIβ, PLCβ1, and PLCβ4 did not change throughout development. In contrast, the expression of GABAAα1a, PSD-95, αCaMKII, synGAP and synaptophysin peaked from 3 weeks onwards. DR from birth prevented developmental down-regulation of NR2B and up-regulation of NR2A subunits. In addition, DR from birth increased the expression of GABAAα1a subunits while the expression of synaptophysin was reduced. It appears that DR activates mechanisms associated with both excitatory and inhibitory pathways so as to maintain a homeostatic balance.

We also assessed the functional architecture of V1 of cats that had undergone monocular deprivation (MD) by lid suture (under ketamine (30 mg/kg) and xylazine (4 mg/kg) anaesthesia i.m.) for 2 or 7 days (n=2 or 3 respectively). MD for 2 days and 7 days resulted in similar depression of deprived eye responses. In contrast, potentiation of non-deprived eye responses was almost twice as strong after 7 days compared to 2 days of MD. Immunoblotting showed that the AMPA receptor subunit, GluR1, was down-regulated after 2 days of MD while no change in its expression was observed after 7 days of MD relative to control. The expression of αCaMKII was up-regulated after 7 days of MD but not after 2 days of MD while synGAP was down-regulated after 2 days of MD but up-regulated after 7 days of MD relative to control. In contrast to DR, MD regulates signalling molecules downstream of NMDA receptors; it appears that different mechanisms are activated depending on the nature of sensory experience.

Supported by the MRC (G0500186).

Where applicable, the authors confirm that the experiments described here conform with The Physiological Society ethical requirements.

PC12

The peripheral pro- and anti-nociceptive effects of galanin are mediated by activation of GalR2

R. Hulse, D. Wynick and L. Donaldson

Department of Physiology & Pharmacology, University of Bristol, Bristol, UK

The neuropeptide galanin is widely expressed in the central and peripheral nervous systems and has been shown to modulate nociception, with both pro- and anti-nociceptive effects described in a dose-dependent manner (Wiesenfeld-Hallin et al. 1988, 1989). These responses were primarily studied using various spinal cord behavioural and electrophysiological paradigms. In contrast very little work has been done on the peripheral nociceptive roles played by galanin. There are currently three known galanin receptors. GalR1 and GalR2 are both expressed by subsets of sensory neurons in the dorsal root ganglia (Kerekes et al. 2003). The aim of this project was to use a saphenous nerve preparation to study the responses of mechano-sensitive primary afferents to galanin and the GalR2/3 specific agonist Gal2-11.

Extracellular teased fibre recordings were made from the saphenous nerve in deeply anaesthetised naïve rats (250-350g; sodium pentobarbital, induction ~60mg/kg i.p. and maintenance ~20mg.kg-1hr-1 i.v.). Individual nociceptive afferents were identified and characterised (conduction velocity <1m/s, mechanical threshold >1g, not brush sensitive). Nociceptive afferents were classified as galanin "responders" if mechanical responses were affected by close arterial injection of 0.1mM galanin.

Intra-arterial 0.1mM Gal2-11 both increased activity evoked by 26g. mechanical stimulation (n=14, evoked firing rate before Gal2-11 1.82Hz +0.66 vs after Gal2-11 2.69Hz + 0.85 $p<0.05$) and decreased mechanical activation thresholds (n=14, before Gal2-11 18.0g +33.0 vs after Gal2-11 4.0g + 8.0 (median+IQR), $p<0.05$), in a manner similar to the effect of galanin (Hulse et al. 2008). In galanin-responsive nociceptors, low concentrations of (100nM) Gal2-11 administered subcutaneously adjacent to the receptive fields caused a similar effect to Gal2-11 administered intra-arterially, in that mechanically evoked activity was enhanced and mechanical activation thresholds decreased (n=4, before 20.5g +15.5 vs after 2.7g + 3.8, $^{*}p<0.05$) in these nociceptors (i.e. a pronociceptive change). In further experiments, subcutaneous injection of high concentration (10μM) Gal2-11 caused an increase in mechanical activation thresholds (i.e. an anti-nociceptive change) in nociceptive afferents (n=5, before 26.0g + 36.0 vs after Gal2-11 100.0g + 154.00, $p<0.05$).

This study demonstrates that activation of GalR2 in peripheral cutaneous afferent terminals exerts both pro- and anti-nociceptive effects on mechanonociceptors, in a dose-dependent manner.

Wiesenfeld-Hallin Z et al. (1988) Exp. Brain Res 71(3): 663-666.

Wiesenfled-Hallin Z et al. (1989) Neurosci Lett 105(1-2): 149-154.

Kerekes N et al. (2003) Eur J Neurosci 18(11):2957-2966.

Hulse R et al. (2008) IASP poster communication no. 2302.

Supported by the MRC (studentship to RH) and grants from MRC (Prof. D. Wynick).

Where applicable, the authors confirm that the experiments described here conform with The Physiological Society ethical requirements.

PC13

Robotic implementation of inhibition of return; potential insight into the biological equivalent

S. McBride, M. Huelse and M. Lee

Department of Computer Science, Aberystwyth University, Abersytwyth, UK

Inhibition of return (IOR) refers to the suppression of stimuli (object and events) processing where those stimuli have previously (and recently) been the focus of spatial attention. In this sense, it forms the basis of attentional (and thus visual) bias towards novel objects. Although the neural mechanism underpinning IOR is not completely understood, it is well established that the dorsal frontoparietal network, including frontal eye field (FEF) and superior parietal cortex are the primary structures mediating its control. These are some of the many modulatory and affecting structures of the deep superior colliculus (optic tectum in non-mammals), the primary motor structure controlling saccade. Although visual information from the retina starts at the superficial superior colliculus, and there are direct connections between the superior and deep layers (Stein and Meredith, 1991) the former cannot elicit saccade directly (Casagrande et al., 1972). This information has to be subsequently processed by a number of cortical and sub-cortical structures that place it 1) in context of attentional bias within egocentric saliency maps (posterior parietal cortex) (Gottlieb, 2007), 2) the aforementioned IOR (Stein et al., 2002), 3) overriding voluntary saccades (frontal eye fields) (Stein and Meredith, 1991) and 4) basal ganglia action selection (McHaffie et al., 2005). Thus, biologically there exists a highly developed, context specific method for facilitating the most appropriate saccade as a form of attention selection.

One of the main problems to overcome in constructing an IOR system is the accurate mapping of the retinotopic space to the global egocentric space i.e. foveated objects within a retinotpoic map must be logged within a global egocentric map to allow subsequent comparison with peripheral retinatopic information. The lateral intraparietal (LIP) region is the primary candidate brain region for this process, given its position in modulating the transfer of visual information from superficial to deep superior colliculus. We present here a working robotic model of an IOR system in the context of static objects using camera pan and tilt information (equivalent to head position) to create a global visual memory. The model potentially provides additional biological insight into the types of information transform and transfer that must take place for an accurate IOR system to exist.

Casagrande, V.A., Diamond, I.T., Harting, J.K., Hall, W.C., Martin, G.F., 1972. Superior colliculus of the tree shrew- structural and functional subdivision into superficial and deep layers. Science 177, 444-447.

Gottlieb, J., 2007. From thought to action: The parietal cortex as a bridge between perception, action, and cognition. Neuron 53, 9-16.

McHaffie, J.G., Stanford, T.R., Stein, B.E., Coizet, W., Redgrave, P., 2005. Subcortical loops through the basal ganglia. Trends in Neurosciences 28, 401-407.

Stein, B.E., Meredith, M.A., 1991. Functional organization of the superior colliculus, in: A.G., L. (Ed.), The neural bases if visual function, Macmillan,, Hampshire, pp. 85-100.

Stein, B.E., Wallace, M.W., Stanford, T.R., Jiang, W., 2002. Cortex governs multisensory integration in the midbrain. Neuroscientist 8, 306-314.

Where applicable, the authors confirm that the experiments described here conform with The Physiological Society ethical requirements.

PC14

Dentate gyrus granule cell firing patterns can induce mossy fibre long-term potentiation *in vitro*

R. Mistry[1], M. Frerking[2] and J. Mellor[1]

[1]MRC Centre for Synaptic Plasticity, Bristol University, Bristol, UK and [2]Behavioral Neuroscience, Univeristy of Health and Science University, Beaverton, OR, USA

Hippocampal granule cells transmit information about behaviourally-relevant stimuli to CA3 pyramidal cells via mossy fibre synapses. These synapses express a form of long-term potentiation (LTP) that is non-Hebbian and does not require NMDA receptors (Nicoll and Schmitz, 2005). Mossy fiber LTP is thought to be induced and expressed presynaptically, hence, the major determinant of whether LTP occurs is activity in the granule cells. However, it remains unclear whether mossy fiber LTP can be induced by activity patterns that granule cells exhibit in vivo, and—if so—what context generates these patterns. To address these issues, we examined granule cell activity from in vivo recordings of 68 granule cells performed previously during performance of a delayed nonmatch-to-sample (DNMS) task (Wiebe and Staubli, 1999, 2001) and found that granule cells exhibit a wide range of spike patterns. We next performed In vitro experiments using extracellular field potential recordings of mossy fibre synaptic transmission in 500μm thick transverse hippocampal slices. These experiments revealed that some, but not all, of the in vivo recorded granule cell spike patterns could induce LTP (3 out of 6 tested). By further defining the activity thresholds for mfLTP in hippocampal slices, we found that mfLTP can only be induced by spike patterns that fire in high frequency bursts (>10Hz) with a low average firing frequency (<0.33Hz). Using this information, we then screened for supra-threshold bursts of activity during the DNMS task. In a subset of cells, supra-threshold bursts occurred preferentially during the sampling phase of the task. If supra-threshold bursting took place later, during the delay phase, task performance was disrupted. We conclude that mfLTP can be induced by granule cell spike patterns during a memory task, and that the timing of mfLTP induction can predict task performance.

Nicoll RA, Schmitz D. 2005. Synaptic plasticity at hippocampal mossy fibre synapses. Nat Rev Neurosci 6(11):863-76.

Wiebe SP, Staubli UV. 1999. Dynamic filtering of recognition memory codes in the hippocampus. J Neurosci 19(23):10562-74.

Wiebe SP, Staubli UV. 2001. Recognition memory correlates of hippocampal theta cells. J Neurosci 21(11):3955-67.

Medical Research Council, ENI-NET (EU), NIH.

Where applicable, the authors confirm that the experiments described here conform with The Physiological Society ethical requirements.

PC15

Properties of neuronal networks linked to nociceptive and non-nociceptive sensory processing in the rat spinal dorsal horn: a study using micro-electrode array technology

R. Chapman[1], D. Ursu[2], E. Sher[2] and A.E. King[1]

[1]IMSB, University of Leeds, Leeds, UK and [2]Eli Lilly & Co., Windlesham, UK

Spinal cord dorsal horn neurones (DHNs) are important for local processing and modulation of somatosensory inputs of peripheral origin. DHN output is determined by the complex interplay of cell biophysical properties, synaptic and network-based mechanisms. Single microelectrode techniques have provided much data on DHN firing patterns and synaptic transmission but little is known about how DHNs are organized and operate as networks to support sensory processing. Multisite-microelectrode array (MEA) technology enables simultaneous recordings from spatially distinct regions within the superficial and deep DH thereby enabling analysis of spatio-temporal characteristics of activity across DH laminae. We have used 4-aminopyridine (4-AP), which triggers network-based activity within the substantia gelatinosa (Chapman *et al.*, 2009, J. Physiol. 587.11: 2499-2510), and MEA technology to generate a map of 4-AP-induced activity and characterise more fully the patterns of network behaviour emergent from nociceptive and non-nociceptive circuitry in vitro.

Transverse lumbar spinal slices (250μm), cut from terminally anaesthetized (urethane, 2g/kg I.P.) Wistar rats, were mounted onto 8 x 8 arrays of 3-D microelectrodes (40μm diameter; 35-45μm height; 100 or 200μm spaced; Ayanda Biosystems) and recordings were performed at 10000 KHz using the Multichannel MEA system. All animal procedures accord with current UK legislation. A digital image of the spinal slice was captured and superimposed onto the 8 x 8 array to indicate precise recording localizations. Spinal cord slices were superfused with oxygenated ACSF at 34°C, and in ACSF containing 4-AP (50μM, n = 28). In control ACSF, little activity was recorded although spontaneous single unit activity (amplitude 25-35μV) was observed in 9 slices at ~8% of recording sites, increasing to ~15% after 4-AP. Superfusion of 4-AP induced widespread excitation that manifest as large amplitude extracellular population field potentials (amplitude range 20-150μV, duration ~407s, peak frequency ~0.8Hz) spatio-temporally distributed throughout the DH. Auto- and cross-correlation analysis respectively revealed a) a rhythmic characteristic to 4-AP-induced activity, as indicated by a narrow range of inter-spike intervals (1.5-4s) and b) a high degree of unilateral synchrony between superficial and deep DH laminae within each hemicord.

These data indicate the potential of MEA technology to describe in more detail the spatial patterns of multi-cell activity in DH networks that support sensory processing including nociception.

Financially supported by BBSRC and Eli Lilly & Co.

Where applicable, the authors confirm that the experiments described here conform with The Physiological Society ethical requirements.

PC16

Responses of lamina I NK1 receptor-expressing projection neurons and interneurons to noxious stimulation

K.S. Al Ghamdi, E. Polgár and A.J. Todd

Department of Neuroscience and Molecular Pharmacology, University of Glasgow, Glasgow, UK

The neurokinin 1 receptor (NK1r), which is the main target for substance P, is expressed by many neurons in lamina I of the spinal dorsal horn, and these show a bimodal size distribution (1). The first part of this study tested the hypothesis that large NK1r-immunoreactive cells in this lamina are projection neurons, while the small cells are interneurons. In the second part, these findings were used to investigate phosphorylation of extracellular signal-regulated kinases (ERK) in projection neurons following noxious stimulation.

To test whether large NK1r-immunoreactive lamina I cells are projection neurons, 3 male Wistar rats were anaesthetised (2-4% isoflurane inhalation) and received injections of cholera toxin B subunit and Fluorogold into caudal ventrolateral medulla and lateral parabrachial area, respectively. Injections into these sites are likely to label all contralateral lamina I projection neurons (2). After 3 days the rats were re-anaesthetized with pentobarbitone (1g.kg^{-1} i.p.) and perfused with fixative. Brain sections were used to reveal spread of tracers, while horizontal sections from L4 segments were immunoreacted for the tracers and NK1r. To investigate responses to noxious stimuli, 3 further rats were anaesthetised with urethane (1.3g.kg^{-1} i.p.) and the skin of the left hindpaw was pinched at 12 locations. After 5 minutes they were perfused with fixative. Horizontal sections of L3-L5 segments were immunoreacted to reveal NK1r, gephyrin and phospho-ERK (pERK). Sections were scanned with a confocal microscope and analysed with Neurolucida software (MBF).

In the retrograde tracing experiments, we analysed 1341 NK1r-positive cells, of which 441 were retrogradely labelled. Cross-sectional soma areas of projection neurons (128-1198 μm^2, median 298 μm^2) were larger than those of cells that were not retrogradely labelled (61-568 μm^2, median 124 μm^2). This difference was highly significant ($P<0.0001$, Mann-Whitney U test). Nearly all (99.4%) of the NK1r cells that were not retrogradely labelled had soma areas <200 μm^2. In contrast, only 9.8% of retrogradely labelled NK1r cells had somata <200 μm^2 and only 0.4% were <160 μm^2.

After applying the noxious pinch stimulus, 221 NK1r-positive lamina I cells were analyzed, of which 91 had soma areas >200 μm^2 and were presumed to be projection neurons. pERK was detected in significantly more of these cells (70.3%) than of the small cells (20.8%; $p<0.0001$, Chi square test). We also examined responses of lamina I projection cells that lack NK1r and have a high density of gephyrin-positive synapses (3) and found that most (62/73, 84.9%) were pERK-positive.These results indicate that NK1r-immunoreactive projection neurons and interneurons in lamina I can be distinguished based on soma size and suggest that relatively more of the projection neurons are activated by noxious pinch stimuli.

Cheunsuang O & Morris R (2000). *Neuroscience* **97**, 335-345.

Spike RC *et al.* (2003). *Eur J Neurosci* **18**, 2433–2448.

Puskár Z *et al.* (2001). *Neuroscience* **102**, 167–176.

Where applicable, the authors confirm that the experiments described here conform with The Physiological Society ethical requirements.

PC17

S100B is superior to neurone specific enolase as a prognostic marker for brain damage following technical knockouts

J.S. Baker[1], P.J. Evans[2], B. Davies[3], S.M. Cooper[4], N.E. Thomas[5], T. Myers[6] and M.R. Graham[6,3]

[1]Health & Exercise Science Research Unit, University of the West of Scotland, Hamilton, Scotland, UK, [2]Department of Endocrinology, Royal Gwent Hospital, Newport, UK, [3]HESAS, University of Glamorgan, Pontypridd, UK, [4]Cardiff School of Sport, UWIC, Cardiff, UK, [5]Centre for Child Research, Swansea University, Swansea, UK and [6]PESS, Newman, Birmingham, UK

Neurobiochemical markers of brain damage, S100B and neurone specific enolase (NSE) have increased in interest in diagnostic clinical neurotraumatology (Herrmann et al., 2001). Serum S-100B is superior to NSE as an early prognostic biomarker for neurological outcome following cardiopulmonary resuscitation (Shinozaki et al., 2009).

The aim of the study was to determine if S100B was a better indicator of neurological trauma than NSE by examining increased serum concentrations following technical knockouts (TKOs) in full contact karate.

Twenty four full contact karate practitioners were divided into three groups retrospectively, post-combat: Technical Knockouts (TKO), (n=6, mean ± SD, age 33.5 ± 3.8 years), Kicks to The Head (KTH) (n=6, mean ± SD, age 27.3 ± 7.8 years), and Kicks to The Body (KTB) (n=12, mean ± SD, age 28.2 ± 6.5 years). The TKO and KTH groups both received direct kicks to the head, while group KTB received only blows to the body. Blood samples were taken before and immediately after combat for analysis of S-100B and NSE. In addition muscle damage was assessed by analysis of serum total creatine kinase (CK) and serum troponin was analysed to exclude cardiac muscle damage.

Significant increases in serum concentrations of S-100B ($p<0.05$) were found immediately after combat within the TKO group (0.16 ± 0.25 vs 0.42 ± 0.39, μg.L-1). There were also significant differences ($p<0.05$) found between TKO, KTH and KTB groups (0.42 ± 0.39 vs 0.32 ± 0.14 vs 0.12 ± 0.16, μg.L-1). Significant increases ($p<0.05$) in NSE occurred only after combat in the TKO group (11.9 ± 5.9 vs 20.2 ± 11.4 ng.ml-1). There were significant increases ($p<0.05$) in CK in both the KTH and KTB groups post combat (KTH: 115.3 ± 61.4 vs 206.3 ± 131; KTB: 159.9 ± 88 vs 189.4 ± 99 U.L-1).

Changes in concentrations of S-100B and NSE suggest TKOs involving head kicks in full contact karate cause biochemically discernible damage of brain tissue. However, S-100B proved more sensitive than NSE, despite both concentrations of analytes being elevated following head kicks not severe enough to result in a TKO, NSE was not elevated compared with kicks to the body. The severity of traumatic brain injury is associated with the early post-traumatic release of protein S-100B and NSE. S-100B is not affected by haemolysis and remains stable for several hours without the need for immediate analysis. Its short half-life and early kinetics of S100B after traumatic brain injury make measurements crucial in the accident and emergency care environment (Korfias et al., 2007). The first serum S-100B would appear to be more reliable as an early predictor of poor neurological outcome than NSE within 24 hours (Woertgen et al., 1997) and can reduce the need for CT scans or admission by over 30% (Springborg et al., 2009).

Herrmann M et al. (2001). J Neurol Neurosurg Psychiatry 70, 95-100.

Korfias S et al. (2007). Intensive Care Med 33, 255-260.

Shinozaki K, et al. (2009). Resuscitation 80, 870-875.

Springborg JB, et al. (2009). Ugeskr Laeger 171, 978-981.

Woertgen C, et al. (1997). Acta Neurochir (Wien) 139, 161-1164.

Morriston Hospital, Swansea.

Where applicable, the authors confirm that the experiments described here conform with The Physiological Society ethical requirements.

PC18

Spinocerebellar ataxia type 17: vocal cord and respiratory system dysfunctions in transgenic mouse model

C. Wu, H. Hsieh-Li, J. Hwang, C. Lin, M. Lin, I. Lu, Y. Fang and G. Lee-Chen

Department of Life Science, National Taiwan Normal University, Taipei, Taiwan

Expansion of the CAG repeat of the TATA-box binding protein (TBP) gene has been identified as the causative mutations in spinocerebellar ataxia 17 (SCA17). TBP is ubiquitously expressed in both central nervous system and peripheral tissues. In addition to SCA patients, mildly expanded alleles were also reported in patients with multiple system atrophy (MSA) and schizophrenia (Chen et al. 2005; Lin et al. 2007). Dysphonia and dysphagia were frequently observed in MSA patients (Shiba & Isono, 2006; Lin et al. 2007). To study the underlying molecular mechanisms, we expressed TBP cDNA containing normal 36 and expanded 61~109 CAG repeats in human embryonic kidney 293 cells. The expanded TBP formed aggregates with significant increase in the cell population at subG1 phase and cleaved caspase-3 (Lee et al. 2009). The TBP constructs were used to establish transgenic (Tg) mouse model with expanded (109 repeats) human TBP overexpression. Two independent Tg lines show ataxia phenotypes after 3 months of age. A significant reduction in the rotarod latency of these mice was identified during the behavioral analysis. As shown in Fig. 1A, respiratory variability was measured using a body plethysmography with the animal sitting quietly, unrestrained and unanesthetised. The respiratory variability of Tg mice was observed on the third weeks after birth and maintained for 6 months. This respiratory variability was stabilized by hypercapnia to a normal level but not affected by low dose of anesthesia. We further studied the activities of the recurrent laryngeal nerve (RLN) and phrenic nerve in response to capsaicin administration (0.625 and 1.25 μg/kg) simultaneously in anesthetized and ventilated Tg mice (Lu et al. 2005). Animals were treated with atropine (0.5 mg/kg, i.p.) first and then with urethane (1.2 g/kg, i.p.). A blunted response of the RLN activity to capsaicin challenge was seen in Tg mice versus wild-type, suggesting that the adduction of the vocal folds might have been malfunctioned. These results may provide a potential strategy of drug development for ameliorating the symptom of dysphonia and dysphagia in SCA17 patients.

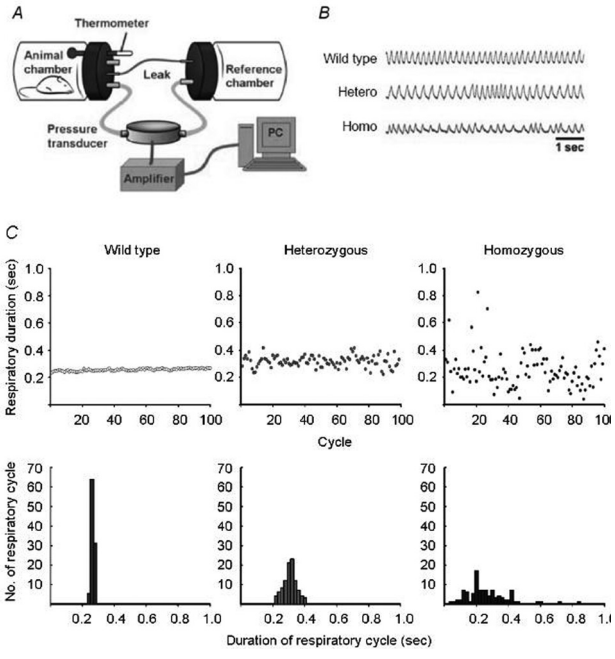

Figure 1. Respiratory variation of SCA17 Tg mice

A, diagram of body plethysmography with animal sat quietly inside the animal chamber connected with the reference chamber via a leaky tubing. The pressure fluctuation which reflects the respiratory activity of the animal was recorded by a differential pressure transducer connected to an amplifier and then stored in a personal computer (PC) via the PowerLab system. B, examples of respiratory activities taken from wild type, heterozygous and homozygous Tg mice. Homozygous Tg mice displayed more variation in respiratory pattern than that of the wild type and heterozygous Tg mice. C, respiratory duration and respiratory cycle frequency histograms recorded from wild type, heterozygous and homozygous Tg mice by analyzing 100 consecutive respiratory cycles during quiet breathing. The large dispersion of respiratory duration was seen in both heterozygous and homozygous Tg mice.

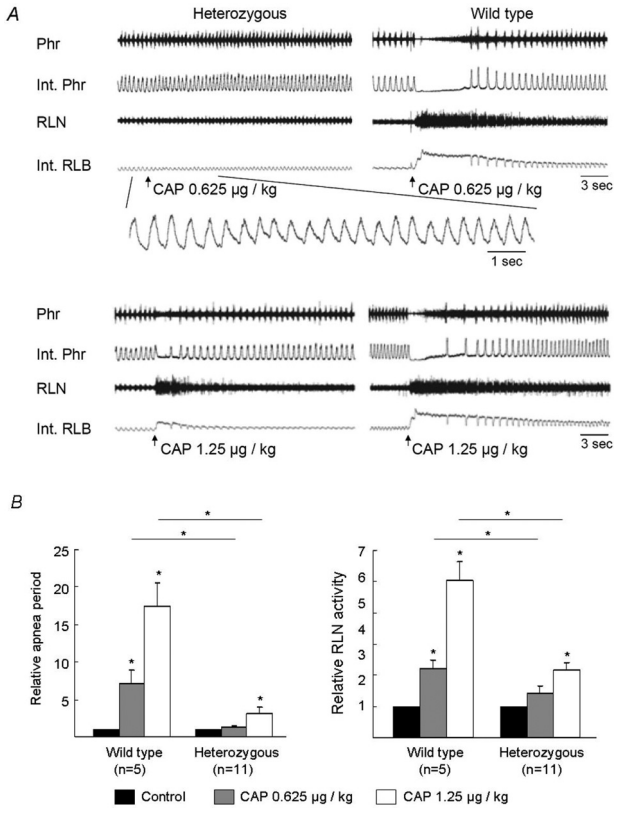

Figure 2. Effect of capsaicin administration on RLN activity

A, the RLN activity was enhanced during apnea and the period of recovery from apnea induced by capsaicin in wild type animals, while was mild in SCA17 heterozygous Tg mice. Int.: integrated, Phr: phrenic nerve activity, RLN: recurrent laryngeal nerve activity, CAP: capsaicin. B, relative apnea period and RLN activity with capsaicin administration. Prolongation of apnea and enhancement of RLN activity in wild-type animals were dose-dependent and significantly larger than those seen in SCA17 heterozygous Tg mice.

Chen CM, Lane HY, Wu YR, Ro LS, Chen FL, Hung WL, Hou YT, Lin CY, Huang SY, Chen IC, Soong BW, Li ML, Hsieh-Li HM, Su MT & Lee-Chen GJ (2005). Schizophr Res 78, 131–136.

Lee LC, Chen CM, Chen FL, Lin PY, Hsiao YC, Wang PR, Su MT, Hsieh-Li HM, Hwang JC, Wu CH, Lee GC, Singh S, Lin Y, Hsieh SY, Lee-Chen GJ & Lin JY (2009). Clin Chim Acta 400, 56–62.

Lin IS, Wu RM, Lee-Chen GJ, Shan DE & Gwinn-Hardy K (2007). Parkinsonism Relat Disord 13, 246–249.

Lu IJ, Lee KZ & Hwang JC (2006). J Appl Physiol 101, 1104–1112.

Shiba K & Isono S (2006). Auris Nasus Larynx 33, 295–298.

This work was supported by grants NSC 95-2320-B-003-002, NSC97-2311-B-003-005-MY3 and NSC97-2311-B-003-008-MY3 from the National Science Council, Executive Yuan, and 96TOP001 from National Taiwan Normal University, Taipei, Taiwan.

Where applicable, the authors confirm that the experiments described here conform with The Physiological Society ethical requirements.

PC19

Acute destabilization of synaptic AMPA receptors with multivalent PDZ ligands

C.M. Tigaret[1,2], M. Sainlos[2], C. Poujol[3], B. Imperiali[4] and D. Choquet[2]

[1]Department of Anatomy, University of Bristol, Bristol, UK, [2]Physiologie Cellulaire de la synapse, UMR 5091, CNRS, Univ. Bordeaux 2, Bordeaux, France, [3]PICIN/Inst. Francois Magendie, Univ. Bordeaux 2, Bordeaux, France and [4]Department of Chemistry, Massachusetts Institute of Technology, Cambridge, MA, USA

The synaptic stabilization of AMPA receptors critically depends on the C-terminal interactions of Stargazin (STG) / transmembrane AMPA receptor regulatory protein (TARP) family members with postsynaptic PDZ domain-containing scaffold MAGUK proteins such as PSD-95 (Nicoll *et al.*, 2006, Bats *et al.*, 2007). To investigate the role of these interactions in the dynamics of AMPA receptors synaptic residency we developed biomimetic competing ligands assembled from two PDZ domain-binding motifs of STG.

Characterization of the ligands in a cellular fluorescence resonance energy transfer/fluorescence lifetime imaging microscopy (FRET/FLIM) system with PSD-95::GFP as donor and STG::mCherry as acceptor revealed an increased affinity for multiple PDZ domains and strong cooperative interaction with PSD-95 (Hill coefficients of 1.378 and 0.9 respectively, for divalent and monovalent ligands).

In cultured hippocampal neurons from Wistar E19 rat pups, the divalent PDZ domain ligands competed with endogenous TARP for the intracellular MAGUK. Incubation for five minutes with membrane permeable ligands (5 μM TAT-$[STG_{15}]_2$) acutely increased the lateral diffusion (median diffusion rate 0.059 $\mu m^2/s$, IQR = 0.021 – 0.16 $\mu m^2/s$, n=1000 trajectories, vs. 0.018 $\mu m^2/s$, IQR = 0.049 – 0.11 $\mu m^2/s$, n=604 trajectories, in control). The effect was transient, peaking at five minutes (mean ± SEM synaptic and extrasynaptic mobile fractions, TAT-$[STG_{15}]_2$: 55.51 ± 3.23%, and 88.21 ± 2.74%, n=7 cells; control: 33.94 ± 5% and 62.96 ± 5.9%, n=8 cells) and disappeared ten minutes after ligand application. This time course was probably due to the entry of mobile AMPARs freed from their PSD-95 anchor in the endocytic pathway, where they would appear as immobile. Indeed, incubation of neurons with TAT-$[STG_{15}]_2$ for 10 min markedly increased the fraction of internalized AMPA receptors (mean ± SEM, 0.84 ± 0.047, n=6 cells vs 0.23 ± 0.06 in controls, n=5 cells).

Intracellular delivery of 50 μM $[STG_{15}]_2$ via patch pipettes induced a rundown of AMPA receptor-mediated EPSCs in synaptically coupled neurons. The rundown was progressive and

reached equilibrium after 20 minutes at 45 ± 4% of the amplitude during the first minute of recording (n=9). The amplitude of NMDA receptor-mediated EPSCs was not affected. $[STG_{15}]_2$ also induced a progressive rundown of AMPA receptor-mediated miniature EPSCs (mEPSC), that equilibrated after 25 minutes, at 76.7 ± 4% (mean ± SEM, n=6) of the amplitude during the first minute of recording.

These results provide evidence for a model in which the TARP-containing AMPA receptors are stabilized at the synapse by engaging in multivalent interactions with the PDZ domain-containing scaffold proteins. In addition, our data suggest the presence of multiple populations of synaptic AMPA receptors that differ in their degree of stabilization.

Nicoll, R.A., Tomita, S. & Bredt, D.S. Auxiliary subunits assist AMPA-type glutamate receptors. Science 311, 1253-1256 (2006).

Bats, C., Groc, L. & Choquet, D. The interaction between Stargazin and PSD-95 regulates AMPA receptor surface trafficking. Neuron 53, 719-734 (2007).

Where applicable, the authors confirm that the experiments described here conform with The Physiological Society ethical requirements.

PC20

Electrophysiological mapping of novel periaqueductal grey – cerebellar pathways

J. Leith, B.M. Lumb and R. Apps

Department of Physiology & Pharmacology, University of Bristol, Bristol, UK

The midbrain periaqueductal grey (PAG) is hypothesised to coordinate behavioural strategies that are dynamically activated under different environmental conditions (Lovick & Bandler, 2005). Stimulation of the ventrolateral (VL) PAG is associated with antinociception, hypotension, bradycardia, and immobility, together termed passive coping (Keay & Bandler, 2001). The sensory and autonomic consequences of PAG activation have received much attention, however the interaction of the PAG with motor control centres necessary to evoke distinct effects on movement remains poorly understood. The aim of this study was therefore to examine whether a functional link exits between the VL-PAG and the cerebellum, the largest sensorimotor structure in the brain, by examining local field potentials and single unit activity in the cerebellar cortex evoked by electrical stimulation of the VL-PAG.

Experiments were carried out in pentobarbitone-anaesthetised (60mg/kg i.p.) adult male Wistar rats (n=7). Craniotomies were performed to allow access to the PAG with a bipolar stimulating electrode and to the posterior cerebellum with a recording electrode. Electrical stimulation of the VL-PAG evoked a distinct field potential on the cerebellar cortical surface. The response had a mean onset latency of 14.5±0.2ms (mean±s.e.m.), and was localised to vermal lobule VIII, distributed bilaterally. The evoked response displayed features typical of climbing fibre fields. In some experiments, single unit recordings were also made from the cerebellar cortex of vermal lobule VIII and VL-PAG stimulation elicited complex spike activity in Purkinje cells at a latency similar to the evoked field. These experiments therefore indicate that a neural pathway exists that links the VL-PAG with the cerebellum via the inferior olive climbing fibre system. We suggest that this novel PAG-cerebellar link may be involved in coordinating behavioural responses associated with VL-PAG function.

Lovick & Bandler (2005) The organisation of the midbrain periaqueductal grey & the integreation of pain behaviours. In: The neurobiology of pain (Hunt & Koltzenburg eds) pp267-86, Oxford UP.

Keay & Bandler (2001) Parallel circuits mediating distinct emotional coping reactions to different types of stress. Neurosci Biobehav Rev 25: 669-678.

BBSRC

Where applicable, the authors confirm that the experiments described here conform with The Physiological Society ethical requirements.

PC21

Orexin-A modulation of lateral habenula neuronal activity

M. Pierucci, M.C. Belle, J. Gigg and H.D. Piggins

Faculty of Life Sciences, University of Manchester, Manchester, UK

The lateral habenula (LHb) plays a key role in linking limbic forebrain and midbrain structures. It is well established that the LHb receives afferent fibres from the lateral hypothalamic area (LHA). Orexin is a neuropeptide involved in promoting arousal state and is expressed by LHA neurons. Orexinergic terminals are present in the LHb, but little is known about this input, in particular, there is no electrophysiological characterization of the effects of orexin on LHb neuronal activity. In order to address this, we recorded extracellular, single-unit activity from Wistar rat LHb brain slices in vitro. Bath application of orexin-A (50, 100 or 300 nM) either inhibited (55/86 of cells tested; >50%) or had a null effect on basal firing rate. To verify whether orexin-A induced inhibition was mediated by GABAergic neurotransmission, gabazine, a GABAA receptor antagonist, was applied to the bath. Blockade of GABAA receptors inhibited a sub-population of LHb neurons (21/40 of tested cells; 50%) and potentiated the inhibitory action of orexin-A when co-applied with the latter. To better understand the effects of orexin on the membrane properties of LHb neurons, we also performed in vitro whole-cell current-clamp recordings from LHb cells. Orexin-A elicited a hyperpolarization in the majority of cells recorded followed in some cases by membrane potential oscillations that triggered bursts of action potentials. Finally, we recorded LHb neurons in vivo in urethane anaesthetised (1.5 g/kg, i.p.) Wistar rats. Consistent with in vitro findings, about half of the cells (22/50 of tested cells) recorded extracellularly in vivo showed a decrease in mean firing rate following intracerebroventricular administration of orexin-A (30 μM or 100 μM). Collectively, these data suggest an inhibitory action of orexin-A on a subpopulation of LHb neurons. Further, since it is well known that orexin receptor activation has an excitatory effect on neuronal activity, it is likely that the effects we observed are mediated by an orexin-dependent recruitment of local GABAergic circuitry.

All procedures were carried out in accordance with the Animal (Scientific Procedures) Act 1986, UK.

Where applicable, the authors confirm that the experiments described here conform with The Physiological Society ethical requirements.

PC22

The involvement of Janus kinase 2 in NMDA receptor-dependent long-term depression in rat hippocampus *in vitro*

C.S. Nicolas[1], S. Peineau[1,2], G. Seaton[3], S.M. Fitzjohn[1], K. Cho[3] and G.L. Collingridge[1]

[1]Department of Anatomy, MRC centre for synaptic plasticity, Bristol, UK, [2]Inserm U676, Hopital Robert Debre, MRC centre for synaptic plasticity, Paris, France and [3]Henry Wellcome L.I.N.E, MRC centre for synaptic plasticity, Bristol, UK

NMDA receptor-dependent long-term depression (LTD) is a major form of synaptic plasticity in the brain that is involved in learning and memory. This form of synaptic plasticity involves an alteration in the efficiency of synaptic transmission mediated by AMPA receptors and depends on NMDA receptor activation. However, little is known concerning the signalling mechanisms leading from NMDA receptor activation to the alteration in AMPA receptor function. We have therefore investigated the potential role of protein kinases in LTD of glutamatergic synaptic transmission in the CA1 hippocampal region. Recently we found that, of approximately 60 ser/thr protein kinases investigated, only GSK-3β (glycogen synthase kinase-3 beta) is involved in LTD (Peineau *et al*, 2009).

We have now investigated the role of tyrosine (tyr) protein kinases in LTD at the CA3:CA1 synapse of hippocampal slices obtained from two-week-old Wistar rats, killed in accordance with the UK Animals (Scientific Procedures) Act 1986. Using whole-cell patch-clamp recordings from CA1 pyramidal cells and tyr kinase inhibitors loaded into the recorded neurones, we have identified the involvement of the Janus kinase (JAK) family in LTD. Thus, NMDA-receptor dependent LTD (63 ± 2% of baseline; n = 28, see Peineau *et al*, 2009) is completely blocked by three different JAK inhibitors: CP690550 (1 μM, 101 ± 2 %; n = 5; $p < 0.05$ compared to control cells), AG490 (10 μM, 97 ± 3 %; n = 6; $p < 0.05$) and JAK inhibitor I (0.1 μM, 99 ± 2 %; n = 6; $p < 0.05$, one-way ANOVA). In contrast, two src-family tyr kinase inhibitors, PP2 (10-20 μM) and SU6656 (10 μM) had no effect on LTD (64 ± 3%; n = 7 and 64 ± 3%; n = 11, respectively).

As JAK2 is the main JAK isoform expressed in the post-synaptic density, we focused on this isoform. We found, using western-blot analysis, that JAK2 is activated in hippocampal slices following NMDA treatment (20 μM, 3 min) and in CA1 dendritic mini-slices following low frequency stimulation (1 Hz, 15 min). Using tyr 1007/1008 phosphorylation of JAK2 as a measure of its activation status, we found an increase of 56 ± 10% (n = 6, $p < 0.05$) and 60 ± 9% (n = 4, $p < 0.05$; paired Student's t test), respectively.

Collectively, these data suggest that activation of JAK2 is required for NMDA receptor-dependent LTD in the hippocampus.

Peineau S *et al.* (2009). Mol. Brain **2**, 22

Where applicable, the authors confirm that the experiments described here conform with The Physiological Society ethical requirements.

PC23

Human olfactory gamma oscillations; correlation with the respiratory cycle

T. Jacob and H. Gunney

School of Biosciences, Cardiff University, Cardiff, UK

Odour-induced olfactory bulb oscillations, called "reactions" by Adrian (1942), were first recorded in the hedgehog in response to clove oil and asafoetida. He reported that an intense stimulus produced a continuous series of small irregular waves with a frequency of 50 Hz. More recently, gamma oscillations (40-100Hz) have been shown to be evoked by olfactory stimulation, particularly during a discrimination task, in mice and rats and are initiated during the inspiratory phase of the respiratory cycle (see review by Kay et al., 2009). In humans, intravenous olfactory stimulation with alinamin has been found to evoke gamma band oscillations at the frontal scalp (Ishimaru et al., 2002). Here, we intended to investigate the presence and nature of gamma oscillations originating in the human olfactory bulb, as well as the influence of the respiratory cycle on these oscillations during periods of odour stimulation. Consenting volunteers were exposed to an odour (vanillin or butyric acid) on a scent card held about 20mm from the nostrils, while we simultaneously recorded the electrical activity at various scalp positions, including N1 (a site at the bridge of nose between the nasion and the medial canthus), using electroencephalography (EEG). Odour stimulation was found to significantly increase the power of gamma-band oscillations at N1 compared to control breathing (t-test, p=0.004). During odour stimulation, respiratory phase was found to have a significant effect on gamma power at N1 (one-way repeated measures ANOVA, $F(1.6,9.7)=7.901$, p=.012; power =.823 at 0.05 significance level). Post hoc analysis showed that gamma power increased significantly in the inspiratory phase upon odour stimulation (LSD (least significant difference), p=0.030), whereas gamma power in the expiratory phase of respiration showed no significant difference upon odour stimulation. This study demonstrates that olfactory induced gamma oscillations can be recorded on the surface of the scalp in humans and we suggest that the observed increase in gamma power in the inspiratory phase reflects odour processing by the olfactory bulb.

Adrian ED (1942). Olfactory reactions in the brain of the hedgehog. J Physiol 100, 459-473.

Ishimaru T et al. (2002). Potential changes with gamma-band oscillation at the frontal scalp elicited by intravenous olfactory stimulation in humans. Chem Senses 27, 711-717.

Kay LM et al. (2009). Olfactory oscillations: the what, how and what for. TiNS 32(4), 207-214.

Where applicable, the authors confirm that the experiments described here conform with The Physiological Society ethical requirements.

PC24

Neuroanatomical features of parvalbumin-expressing neurons in the rodent spinal dorsal horn

D.I. Hughes, C.M. Kinnon and S. Sikander

FBLS, University of Glasgow, Glasgow, UK

Parvalbumin (PV) is expressed in a small proportion of spinal dorsal horn neurons in both the rat and mouse. In the rat, approximately 70% of PV-immunoreactive (-ir) cells in laminae II and III are inhibitory neurons. These comprise a heterogeneous population of cells that contain GABA only, glycine only, or both GABA and glycine, and each sub-population may represent a subtle, functionally distinct class of interneuron. The aims of this study were to i) compare the distribution, morphology and neurochemical phenotype of parvalbumin-expressing neurons in the superficial dorsal horn of rats and mice; ii) determine the main afferent inputs on to these PV-ir cells; iii) identify the postsynaptic targets of these PV-ir cells.

Adult male Wistar rats and ICR mice were terminally anaesthetised by i.p. injection of sodium pentobarbitone prior to perfusion fixation. Transverse or sagittal sections from lumbar segments of the spinal cord were first incubated in a cocktail of primary antibodies and then species-specific secondary antibodies tagged with fluorescent markers to reveal labelling for parvalbumin, vesicular GABA transporter, vesicular glutamate transporter 1 (VGLUT1), IB4, CGRP, HCN channel subunits and PKCγ. Confocal image stacks were collected from representative sections of each animal to determine the morphology of PV-ir cells, the relationships of their axons with primary afferent terminals, the main primary afferent input onto these cells and the proportion of PV-ir cells expressing HCN channel subunits. Image stacks were analysed using Neurolucida image-analysis software.

Although the main plexus of PV-ir cells in the rat and mouse dorsal horn was found in lamina II inner (IIi) and III respectively, the main plexus of PV-ir axons of either species arborised in lamina IIi. PV-ir cells in both species often displayed islet cell-like morphology, with large cell bodies and elongated dendritic arbors extended in the rostro-caudal axis. These cells often expressed immunolabelling for HCN channel subunits, suggesting that PV-containing neurons show Ih currents and display tonic discharge patterns. The main primary afferent input on to these cells comes from IB4–positive terminals, while inhibitory PV-ir axon terminals target VGLUT1-ir axon terminals in lamina IIi almost exclusively.

These results suggest that PV-containing neurons in the superficial dorsal horn of both rats and mice comprise very similar populations. They also show that PV-containing neurons are likely to include islet cells, receive strong afferent input from non-peptidergic C-fibres, are likely to show Ih currents and display tonic discharge patterns, and mediate presynaptic control over myelinated primary afferents from low threshold mechanoreceptor and down-hair afferents.

Where applicable, the authors confirm that the experiments described here conform with The Physiological Society ethical requirements.

PC25

Noxious stimulation evokes delta brushes in human preterm infants

L. Fabrizi[1], R. Slater[1], S. Olhede[2], A. Worley[3], J. Meek[4], S. Boyd[3] and M. Fitzgerald[1]

[1]Department of Neuroscience, Physiology and Pharmacology, University College London, London, UK, [2]Department of Statistical Science, University College London, London, UK, [3]Clinical Neurophysiology, Great Ormond Street Hospital for Children, London, UK and [4]Neonatal Intensive Care Unit, Elizabeth Garrett Anderson and Obstetric Hospital, University College London Hospital, London, UK

Delta brushes are distinctive electroencephalographic (EEG) pattern of premature infants. They appear at 27 weeks, peak around 32-34 weeks and disappear around 44 weeks post-menstrual age (PMA) (1). Endogenous correlated neuronal activity and afferent inputs during prenatal and early postnatal brain development are the key factors of the organization of the functional cortical neuronal networks (2). Delta-brushes in human infants have been reported to be evoked in the controlateral somatosensory cortex by spontaneous limb movements and tactile stimulation, suggesting that they may be the result of a sensory feedback involved in the organization of the somatosensory cortex (3).

While, under normal physiological conditions, sensory inputs are innocuous, premature infants in intensive care are frequently exposed to noxious stimuli, such as clinically required heel lances (4). Such intense and repeated stimulation may interfere with the normal balance of activity-dependent development of somatosensory circuits. If so, we hypothesise that noxious stimulation will alter the normal occurrence of delta-brush activity.

EEG recordings were conducted on 16 premature neonates, 33-37 weeks PMA, born extremely prematurely (24-28 weeks PMA, n = 5) and prematurely (30-37 weeks PMA, n = 11) and on a control population of 7 full term newborns. Electrodes were placed at standard scalp positions according to the international 10-20 system. Five-second epochs, starting 2.5 seconds before event, corresponding to a noxious clinically-essential heel lance, an innocuous touch and no stimulation, were submitted to wavelet time-frequency analysis for automatic delta brush detection.

Noxious stimulation evoked delta brush activity in 69% of the test occasions in premature infants (5/5 if born extremely prematurely and 6/11 if born prematurely), but innocuous touch in only 12% (1/5 and 1/11). Delta brush activity, when evoked by noxious stimulation, was always present in the temporal region (T3/T4) and never at the vertex (CPz/Cz) (9-54% of the times at other electrode sites). The spontaneous occurrence in premature infants was of 18% (0/5 and 3/11) and occurrence following noxious or innocuous stimulation in the control group was 14% (1/7).

Noxious stimulation triggers delta brushes more frequently than innocuous stimulation, especially in the temporal region of the brain. It is therefore possible that noxious stimulation disturbs the normal organization of the somatosensory cortex during development. This is more likely in premature infants that were born extremely prematurely. However it is not clear if this

is due to a longer hospitalization and related exposure to noxious stimuli or to differences in the development of the brain.

F. Torres, C. Anderson, J Clin Neurophysiol 2, 89 (Apr, 1985).

L. C. Katz, C. J. Shatz, Science 274, 1133 (Nov 15, 1996).

M. Milh et al., Cereb Cortex 17, 1582 (Jul, 2007).

A. Taddio, V. Shah, C. Gilbert-MacLeod, J. Katz, JAMA 288, 857 (Aug 21, 2002).

We thank the research nurses D. Patten and J. Yoxen and the clinical physiologist S. Roberts for the data acquisition. This work was supported by the Medical Research Council.

Where applicable, the authors confirm that the experiments described here conform with The Physiological Society ethical requirements.

PC26

Urothelium-derived nitric oxide modulates cholinergic responses in the body of the rat urinary bladder but not in the trigonum

G. Tobin and U.K. Killi

Department of Pharmacology, Neuroscience and Physiology, the Sahlgrenska Academy at University of Gothenburg, Gothenburg, Sweden

In the urinary bladder, nitric oxide (NO) influences efferent and afferent neurotransmission (Alfieri et al., 2001; Giglio et al., 2005). In patients suffering from interstitial cystitis, afferent pathways are sensitized and the release of NO is associated with the condition. In cyclophosphamide (CYP)-induced cystitis in the rat, an upregulation of muscarinic M5 receptors occurs, particularly in the urothelium, together with an increase in endothelial NOS expression in the submucosa/mucosa (Giglio et al., 2005). The current study aimed to explore the tissue origin of NO in the normal and inflamed urinary bladder and to compare in vitro findings with effects in in vivo conditions. With local ethics committee approval, male rats were either pre-treated with saline or CYP (100 mg/kg) intraperitoneally and 48–60 h later, the bladder function was examined in in vitro and in in vivo (anaesthetized (Ketalar 50 mg/kg combined with Domitor 0.3 mg/kg i.p.) and conscious rats) experiments. In the CYP-pretreated rats, the contractile in vitro response to methacholine was substantially reduced in muscle strip preparations from the bladder body but not in strips from the trigonum. In normal detrusor preparations, the nitric oxide synthase inhibitor N-ω-nitro-L-arginine (L-NNA; 10-4 M) increased the cholinergic contractile effect, while it had no effect on trigonal muscle strips. In inflamed body preparations, the L-NNA effect was substantially larger than in the normal preparations. The administration of 4-diphenylacetoxy-N-methylpiperidine (4-DAMP; 10-8 M) enhanced the carbachol-induced contractile responses of inflamed strips but not in normal strips. In anaesthetized rats, methacholine induced smaller contractions (i.e. bladder pressure increases) in inflamed bladders than in controls. The removal of the urothelium did not affect the cholinergic contractions in normal bladders, while it enhanced them in inflamed bladders. The NO synthase inhibitor Nω-nitro-L-arginine methyl ester (L-NAME; 30mg/kg i.v.) caused the methacholine-evoked contractions to be of similar magnitude in urothelium-denuded inflamed bladders as in intact inflamed bladders. In conscious rats, assessing the urodynamics in a metabolic cage, voiding volumes were significantly lower in CYP pre-treated than in saline pre-treated rats. Neither 4-DAMP nor L-NAME had any effect in the normal rats. In CYP pre-treated rats, both 4-DAMP and L-NAME significantly increased voiding volumes.

Conclusions: In CYP-induced cystitis, the cholinergic function of the bladder is altered in the bladder body but not in the trigonum. The changes of the cholinergic effects, involving the production of NO presumably occur in the urothelium. The in vitro findings are supported by in vivo findings in anaesthetized as well as in conscious rats.

Alfieri AB, Malave A & Cubeddu LX. (2001). Nitric oxide synthases and cyclophosphamide-induced cystitis in rats. Naunyn Schmiedebergs Arch Pharmacol 363, 353-357.

Giglio D, Ryberg AT, To K, Delbro DS & Tobin G. (2005). Altered muscarinic receptor subtype expression and functional responses in cyclophosphamide induced cystitis in rats. Auton Neurosci 122, 9-20.

This study was supported by grants from Wilhelm och Martina Lundgrens Vetenskapsfond.

Where applicable, the authors confirm that the experiments described here conform with The Physiological Society ethical requirements.

PC27

Does the extended amygdala contain autonomous circadian oscillators?

A.T. Hughes, C. Guilding, L. Schmidt and H.D. Piggins

Faculty of Life Sciences, University of Manchester, Manchester, UK

A number of recent *in vivo* studies have reported rhythmic expression of the core circadian clock gene protein, PER2, in nuclei of the extended amygdala complex[1,2], raising the intriguing possibility that these areas contain circadian oscillators. In order to determine the presence and properties of potential autonomous circadian oscillators in the central nucleus of the amygdala (CeA), basolateral nucleus of the amygdala (BLA) and oval nucleus of the bed nucleus of the stria terminalis (ov-BNST), we cultured isolated samples of these amygdala nuclei. Coronal brain slice cultures were made from each of these areas from adult male mice expressing a PER2::luciferase fusion protein reporter. PER2-driven luminescence expression was either tracked using photomultiplier tube assemblies (PMTs) or visualised on a highly sensitive Olympus LV200 luminescence microscope using photovideomicroscopy. Brain slice cultures from the CeA and ov-BNST expressed a single peak in PER2 expression which diminished to background levels after approximately 24h *in vitro*. Damped PER2 expression in the CeA and ov-BNST could be induced by treatment with corticosterone at 30ng/ml. No endogenously driven expression of PER2 was detected in isolated cultures of BLA, though PER2 could be induced in cultures from this area with 30ng/ml corticosterone. These data demonstrate that none of the nuclei of the extended amygdala examined here contain autonomous circadian oscillators and

that rhythmic activity in these nuclei *in vivo* must be driven by systemic signals or inputs from other brain areas.

Amir *et al.* (2004). *J Neurosci* **24**, 781-790.

Waddington Lamont *et al.* (2005). *PNAS* **102**, 4180-4184.

Sponsored by the Biotechnology and Biological Sciences Research Council.

Where applicable, the authors confirm that the experiments described here conform with The Physiological Society ethical requirements.

PC28

Cerebral capillary "stress-failure" in non-fatal high-altitude cerebral oedema

D.M. Bailey[1], K. Kallenberg[2], C. Dehnert[3], A. Dörfler[4], P.D. Schellinger[4], M. Knauth[2] and P. Bärtsch[3]

[1]Faculty of Health, Science and Sport, University of Glamorgan, South Wales, UK, [2]Department of Neuroradiology, Georg August University Medical Centre, G√∂ttingen, Germany, [3]Department of Internal Medicine, University of Heidelberg, Heidelberg, Germany and [4]Department of Neuroradiology, University Medical Centre, Erlangen, Germany

Acute mountain sickness (AMS) is a neurological syndrome triggered by the hypoxia of high-altitude that is characterised by headache and associated vegetative symptoms. It has traditionally been considered a self-limiting form of high-altitude cerebral oedema (HACE) with both syndromes sharing a common pathophysiology linked by vasogenic oedematous brain swelling that ultimately leads to intracranial hypertension (Hackett and Roach, 2001). However, recent studies have consistently failed to identify "gross" blood-brain barrier (BBB) disruption as a distinguishing event (Bailey *et al*., 2006, 2009a; Kallenberg *et al*., 2008). In contrast, severe vasogenic oedema and micro-haemorrhages are characteristic features of HACE, a life-threatening condition defined by severe truncal ataxia and clouded consciousness.

To confirm these subtle structural differences across the spectrum of illness, we hypothesised that unlike subjects with severe AMS, the brains of HACE survivors would be characterised by an accumulation of insoluble iron (III) oxide-hydroxide in the form of haemosiderin deposits that we would take to reflect cerebral capillary "stress-failure" subsequent to BBB disruption. A highly-sensitive Susceptibility Weighted Imaging-MRI technique was performed 1.5-31 months following diagnosis in 3 patients who had been rescued having survived HACE (aged 26-66 years) and in 3 control subjects diagnosed with severe AMS (aged 26-47 years) following comparable altitude exposure. Multiple haemosiderin deposits indicative of micro-haemorrhages were found predominantly within the corpus callosum (corpus, splenum and genu) of HACE patients whereas no deposits were present in the AMS subjects. Additional diffusion-weighted (ADC mapping) combined with FLAIR imaging confirmed the persistence of vasogenic oedema in one subject diagnosed with HACE 6 weeks previously.

These findings are the first to identify haemosiderin deposits within the corpus callosum as a novel diagnostic biomarker that distinguishes HACE from AMS. Since AMS has been associated with impaired cerebral autoregulation (Bailey *et al*., 2009b), the more severe arterial hypoxaemia characteristic of HACE may, in the setting of hypoxic cerebral vasodilatation, force a pressure-passive increase in cerebral blood flow and capillary hydrostatic pressure that ultimately leads to mechanical failure of the BBB. The long-term neurological impact of capillary stress-failure within the corpus callosum of HACE survivors remains to be examined.

Bailey DM *et al*. (2006). *J. Cereb. Blood. Flow. Metab*. **26**, 99-111.

Bailey DM *et al*. (2009a). *Am. J. Physiol. Regul. Integr. Comp. Physiol* (**epub**:10.1152/ajpregu.00366.2009)

Bailey DM *et al*. (2009b). *J. Physiol*. **15**, 73-85.

Hackett PH and Roach RC. (2001). *New Eng J Med* **345**, 107-114.

Where applicable, the authors confirm that the experiments described here conform with The Physiological Society ethical requirements.

PC29

Effects of *Momordica charantia* fruit extract in the treatment of glioma cancer

G. Manoharan

Pharmacy and Pharmaceutical Science, University of Central Lancashire, Preston, UK

Prior to the availability of chemotherapeutic agents, dietary measures, including traditional medicines derived from plants, were the major forms of cancer treatment1. One such plant is M. charantia (Family: Cucurbitaceae), whose fruit is known as Karela or bitter gourd. M. charantia is believed to posses anti-carcinogenic properties and it can modulate its effect via xenobiotic metabolism and oxidative stress 2, 3. This study characterizes one of the active ingredients of M. charantia and investigates its potential chemotherapeutic effect in glioma cancer therapy. The fruit was washed and cut in to small pieces, liquidised in deionised water using a blender and subsequently, dried using a rota evaporator and an oven. Four different glioma cell lines (1321N1, GOS-3, U87-MG, and WERI-Rb1) and normal L6 skeletal muscle cell line were treated with different concentrations (100 μM, 200 μM, 300 μM, 400 μM) of the crude fruit extract separately for 24 hours using 2500 cells in each 200 μl 96 well plates. In another series of experiment, the crude extract of M. Charantia was used to isolate α and β Momocharin ingredient employing HPLC techniques. The isolated active protein ingredient was subsequently tested in all five cell lines including normal L6 skeletal muscle cells employing different concentrations (200 μM - 800 μM). The cell viability was measured using MTT assay kit for every 8 hrs, 16 hrs and 24 hrs. Initial results have shown that either the crude extract of M. charantia or α and β Momocharin can evoke a significant ($p<0.05$; Student's-t-test) decrease in cell viability for each cell line compared to untreated cells of each cancer cell line. Typically, 800 μM of α and β Momocharin evoked cell death of 40.94 %, 44.39 %, 37.26 % and 57.67 % for 1321N1, GOS-3, U87-MG, WERI-Rb1 cell lines, respectively compared to control (100 %) untreated cells. In contrast, either the crude extract or α and β Momocharin had no significant effect on control L6 skeletal

muscle cell line compared to untreated cells. These effects of crude extract and α and β Momocharin were dose-dependent. In conclusion, the results have shown that both the crude extract and α and β Momocharin can elicit marked anti-cancer effects in different glioma cell lines.

Omar S, et al., (2007). "Hypoglycemic effect of the seeds of Momordica charantia." Fitoterapia 78, 46-47.

Lee-Huang S, Huang PL, Chen HC, et al., (1995). Anti-HIV and anti-tumor activities of recombinant MAP30 from bitter melon. Gene 161, 151-156.

Catherine J, Beth Strifler et al., (1983). In Vivo Antitumor Activity of the Bitter Melon (Momordica charantia). Cancer Research 43, 5151-5155.

Kim J H et al., (2002). "Induction of apoptosis by momordin I in promyelocytic leukaemia (HL-60) cells." Anticancer Res 22, 1885-1889.

M. Gunasekar, R.W. Lea, T. J. Snape and J. Singh.

Where applicable, the authors confirm that the experiments described here conform with The Physiological Society ethical requirements.

PC30

Differential effects of low frequency repetitive stimulation of the major afferent pathways of the rat hippocampal CA3 region *in vivo*

N.A. Vorobyov, G.L. Collingridge and Z.A. Bortolotto

Department of Anatomy, University of Bristol, Bristol, UK

The hippocampal CA3 region receives input directly from the entorhinal cortex via entorhinal-CA3 projections and indirectly through mossy fibres from granule cells of the dentate gyrus (DG). Additionally there are recurrent collaterals projecting ipsi- and contra laterally from CA3 neurons. Here we studied CA3 responses to low frequency (1 - 10 Hz) stimulation of these three inputs, in Wistar rats maintained under Nembutal anaesthesia (50 mg/kg, i.p.). We found the following. 1) Low frequency stimulation of CA3 recurrent collaterals was accompanied by short-term potentiation of CA3 responses followed by their quick return to initial values evoked by basal single stimulation (1/30 sec). This effect was observed following the stimulation of contralateral CA3 or ipsilateral CA1 or inpsilateral hilus fibers. 2) Low frequency stimulation of direct entorhinal inputs to CA3 was accompanied by short-term depression of CA3 responses followed by their quick return to initial values. This was observed during stimulation of the subiculum or molecular layer of the DG. 3) Low frequency stimulation of mossy fibres, by stimulation within the granular layer of the DG, was accompanied by short-term depression followed by long-term potentiation (LTP) of CA3 responses. This effect developed as a rebound: suppressed responses during low frequency stimulation were replaced by enhanced responses during basal stimulation. LTP was observed immediately after the low frequency stimulation protocol. The effects described above were clearly dependent on stimulation frequency (the higher frequency the greater the effect) and were NMDA receptor independent, since all of the experiments were done in the presence of ketamine (10 mg/kg). Thus these results suggest functional differences between the three different CA3 inputs, and identifies a form of NMDA receptor independent LTP, which is induced by low frequency stimulation.

Supported by MRC.

Where applicable, the authors confirm that the experiments described here conform with The Physiological Society ethical requirements.

PC31

Circadian oscillators in the epithalamus

C. Guilding, A.T. Hughes and H.D. Piggins

University of Manchester, Manchester, UK

The lateral habenula (LHb) is implicated in a range of cognitive, emotional and reproductive behaviors, and recently this epithalamic structure was suggested to be a component of the brain's circadian system [1, 2]. Circadian timekeeping is driven in cells by the cyclical activity of core clock genes and proteins such as *per2*/PER2. There are currently no reports of clock gene/protein expression in the habenula and therefore the question of whether this structure has intrinsic timekeeping properties remains unresolved. Here using videomicroscopy imaging and photon-counting of PER2::LUC fusion protein bioluminescence together with multiunit electrophysiological recordings [3], we tested the endogenous circadian properties of the habenula *in vitro*. We show that a damping circadian oscillator is localized primarily to the medial subregion of the mouse LHb. Rhythms in PER2::LUC bioluminescence are visualized in single cells and oscillations continue in the presence of the sodium channel blocker, tetrodotoxin (TTX), demonstrating that individual cells have intrinsic timekeeping properties. Ependymal cells lining the dorsal third ventricle also express circadian oscillations in PER2. These findings establish for the first time that neurons and non-neuronal cells in the epithalamus express rhythms in cellular and molecular activities, indicating a role for circadian oscillators in the temporal regulation of habenula controlled processes and behavior.

Guilding C, Piggins HD (2007). *Eur J Neurosci*, **25**(11), 3195-216.

Tavakoli-Nezhad M, Schwartz WJ (2006). *Chronobiol Int,* **23**(1-2), 217-24.

Guilding C *et al* (2009). *Molecular Brain*, **2**(1), 28.

Supported by the BBSRC and Wellcome Trust.

Where applicable, the authors confirm that the experiments described here conform with The Physiological Society ethical requirements.

PC32

Chaotic neural dynamics as evinced from scalp electroencephalography (EEG)

A. Dube[1], A. Kumar[2], K. Gupta[1], P. Vyas[3], D. Boolchandani[2] and R. Sonania[4]

[1]Physiology, S.M.S. Medical College, Jaipur, Rajasthan, India, [2]Electronics and Communication, Malviya National Institute of Technology, Jaipur, Rajasthan, India, [3]Mathematics, University of Rajasthan, Jaipur, Rajasthan, India and [4]Electronics and Communication, Khaitan Government Polytechnic College, Jaipur, Rajasthan, UK

The objective of the present study was to elucidate evidence of and to revisit chaotic itinerancy in human brains by means of

noninvasive scalp electroencephalogram (EEG) in normal subjects; with the assumed tenet that chaotic itinerancy occurs in sequences of cortical states marked by state transitions that appear as temporal discontinuities in neural activity patterns. The present study was based on unprecedented advances in spatial and temporal resolution of the phase of oscillations in scalp EEG. The EEG data was processed and modeled by the technique of curve fitting and temporal resolution was advanced by the use of Hilbert Transform (in Matlab version 7.0), which re-affirmed the variations in phase and amplitude in all scalp EEG electrical signals from 0 through 99 Hz frequencies. The numerical derivative of the analytic phase revealed plateaus in phase. The plateaus were bracketed by sudden jumps in phase. The widespread synchrony of the jumps in analytic phase manifests a metastable cortical state in accord with the theory of self-organized criticality. The jumps appear to be subcritical bifurcations. They reflect the aperiodic evolution of brain states through sequences of attractors that on access support the experience of remembering. State changes resembling phase transitions occur continually everywhere in cortex. Only the largest and longest-lasting state appears in scalp EEG, giving the appearance of chaotic itinerancy. The $1/f\alpha$ spatial and temporal spectra of scalp EEG denote that brain maintains a state of self-organized criticality (SOC) as the basis of its capacity for rapid adjustment to environmental changes.

Basar E. 2004 Brain and Memory Dynamics. CRC Press LLC.

Freeman WJ. (2000). Neural Networks 13, 11 – 13.

Freeman WJ. (2003). Chaos 13, 1 – 11.

The Principal, S.M.S. Medical College, Jaipur, India.

Professor and Head, Dr. R. C. Gupta, Department of Physiology, S.M.S. Medical College, Jaipur, India.

Professor and Head, Dr. Ashok Pangariya, Department of Neurology, S.M.S. Medical College, Jaipur, India.

Where applicable, the authors confirm that the experiments described here conform with The Physiological Society ethical requirements.

PC34

The accuracy of tactile localization is reduced by skin stretch at the human wrist

F. Cody[1], R. Idrees[1], D. Spilioti[1] and E. Poliakoff[2]

[1]Faculty of Life Sciences, University of Manchester, Manchester, UK and [2]School of Psychological Sciences, University of Manchester, Manchester, UK

The precision of tactile point localization (locognosia, defined by Hamburger, 1980) is greatest for body regions (e.g. hand) whose touch units have small receptive fields (RFs). However, the skin is an elastic organ that is continuously distorted as our limbs move, with fluctuations in RF dimensions. To date, possible associated locognosic changes have not been reported. Therefore, we have tested the hypothesis that tactile localization accuracy is reduced when the skin is distended, with concurrent expansion of RFs.

Twenty-five (22 female, 3 male, aged 18-21 years) healthy subjects participated. A 7-point linear stimulus array (5mm point separation) was drawn on the shaved skin of dorsal surface of the non-dominant wrist, along its longitudinal axis. In each trial, a brief tactile stimulus was first applied, with a von Frey hair (rating 150mN) to the central locus (reference) followed by an identical stimulus (test) to one of the 7 test loci. The subject stated the direction ("more distal" / "more proximal") of the test relative to the reference stimulus. Each test locus received 10 stimuli and the probability of a "more distal" directional response was calculated. The interval of uncertainty (IU, a measure of locognosic discriminatory threshold) was estimated from standard psychophysical functions (probability of directional judgement versus stimulus locus). Spatial locognosic acuity was quantified under baseline conditions (wrist at 0deg) and during application of background skin stretch by (1) controlled flexion (Wrist-Bend, small (35deg) and large (70 deg) amplitude) of the relaxed joint and (2) matched direct pulling on the skin (Skin-Pull, small and large amplitude) using wires attached to adhesive pads.

Statistical analysis of IU using a 2 (amplitude of skin stretch, small, large) x 2 (mode of skin stretch, Wrist-Bend, Skin-Pull) repeated-measures ANOVA showed a significant main effect of stretch amplitude ($F(1,24) = 11.123$, $p = .003$) but no main effect of stretch mode ($F(1,24) = 2.306$, $p = .142$). Paired t-tests indicated that IU was significantly greater (less accurate) than baseline for the two large amplitude stretch conditions (Wrist-Bend $t(24) = 2.445$, $p = .022$; Skin-Pull $t(24) = 2.120$, $p = .045$) but did not differ significantly ($p > .25$) from baseline for either of the small stretch conditions.

We interpret our observations as (1) supporting the long-held assumption that tactile localization depends primarily upon the RF dimensions of regional touch units and (2) suggesting that tonic activation of non-cutaneous proprioceptors during joint positioning exerts rather little modulatory effect.

Hamburger HI (1980). PhD Thesis, University of Amsterdam.

Where applicable, the authors confirm that the experiments described here conform with The Physiological Society ethical requirements.

PC35

Electrophysiological actions of orexin on neurons in the mouse suprachiasmatic nucleus (SCN)

M.D. Belle[1], R.H. Williams[2], D. Burdakov[3] and H.D. Piggins[4]

[1]Faculty of Life Sciences, University of Manchester, Manchester, UK, [2]Department of Pharmacology, University of Cambridge, Cambridge, UK, [3]Department of Pharmacology, University of Cambridge, Cambridge, UK and [4]Faculty of Life Sciences, University of Manchester, Manchester, UK

Endogenous near 24h (circadian) rhythms in physiology and behaviour are generated by the main circadian clock in the hypothalamic suprachiasmatic nucleus (SCN). The synchronization of the SCN clock by environmental light (photic cues) and by stimuli that promote internal arousal (non-photic cues) results in daily rhythms in sleep and wake, core body temperature, etc. Some components of the molecular basis for the SCN

clock (the so-called clock genes/proteins) are well characterized and include the *period 1* (*per1*) gene and its protein product PER1. The major light input pathway to the SCN utilizes glutamate and the effects of glutamate on mouse SCN neurons, including those expressing an enhanced destabilized green fluorescent protein (EGFP) driven by the *per1* promoter are known. The neurochemicals communicating non-photic information to the SCN are less well understood, but there has been considerable interest in the arousal-promoting orexin/hypocretin neuropeptides. Orexin is synthesized by discrete populations of neurons localized mainly in the lateral hypothalamus. Some lateral hypothalamic neurons innervate the SCN region but it is unclear if and how orexins influence SCN neuronal activity, particularly those expressing *per1*. We used whole-cell recordings to investigate the effects of orexin on SCN neurons expressing *per1*::EGFP as well as those neurons in which *per1*::EGFP could not be detected ('*per1*', and 'non-*per1*' neurons, respectively) in SCN brain slices *in vitro*. In the majority (70%) of *per1* and non-*per1* neurons tested, orexin (50-300 nM) induced biphasic responses, causing the membrane potential of the neurons to oscillate. In some of these neurons, co-application of orexin with gabazine (20 μM) suppressed a phasic GABA-mediated hyperpolarization to reveal a subtle orexin-induced depolarization. In 5% of neurons examined, orexin caused membrane depolarization, while in 10% robust hyperpolarization was seen. This orexin-induced hyperpolarization was inhibited by pretreatment with gabazine or tetrodotoxin (500 nM), suggesting that orexin acts presysnaptically to recruit GABAergic interneurons. Voltage-clamp recordings supported this, and revealed a dose-dependent increase in inhibitory postsynaptic current frequency during bath application of orexin that was eliminated by gabazine. We also observed that orexin caused a significantly stronger inhibition ($p< x 10^{-5}$) in night *per1* and non-*per1* neurons when compared with day neurons. This nighttime orexin-induced hyperpolarization in *per1* and non-*per1* neurons was robust (-70 mV) and long lasting(≈45 min). We conclude that orexin has complex effects on SCN neurons that involve the recruitment of local GABAergic interneurons that tonically or phasically inhibit the neurons. These effects had a clear day/night difference.

This work was funded by a project grant from the BBSRC

Where applicable, the authors confirm that the experiments described here conform with The Physiological Society ethical requirements.

PC36

Transformation in the neural code for whisker deflections from receptors to cortex

M. Bale and R.S. Petersen

Faculty of Life Sciences, The University of Manchester, Manchester, UK

A common principle for the organization of sensory systems is a massive expansion in neuronal numbers from the periphery to the cerebral cortex. Neural codes at successive stages of the sensory pathway thus operate under markedly different anatomical constraints. We have investigated how the neural representation of whisker stimulation compares at successive stages of the lemniscal whisker pathway. Although changes in tuning are well documented, changes in reliability have only been investigated by a few studies. We have investigated the variability in neural responses at different levels of the whisker lemniscal pathway by studying both deflections of whiskers in different directions and dynamic whisker stimulation using white noise. We made extracellular single unit recordings under identical experimental conditions in the trigeminal ganglion, ventroposterior medial (VPM) nucleus of the thalamus and barrel cortex of urethanised rats (1.5 g/kg, ip). We found a dramatic decrease in both reliability and the amount of mutual information that single units convey about whisker direction deflection across the pathway. VPM units conveyed 48% of the mutual information conveyed by ganglion units, cortical units 12%. Simultaneously recorded cortical pairs conveyed 2.1 times the information than their constituent single units suggesting cortex may compensate for information loss by population coding. Yet despite the tranformation in the code the first post-stimulus spike at each level transmitted the majority of the information. Transformations in the coding of dynamic whisker stimulation included a decrease in firing rate, a sharp increase in adaptation at the level of barrel cortex and a decrease in spike timing precision along the pathway. The key result was a decrease in the reliability of white noise representation. In sum, these results indicate a shift in coding strategy along the whisker pathway that is optimised for fast and reliable sensory guided behaviour.

M.E. Diamond, R.A.A. Ince, M. Maravall and S. Panzeri for valuable discussions

Where applicable, the authors confirm that the experiments described here conform with The Physiological Society ethical requirements.

PC37

Mechanisms of TRPV1-mediated desensitisation of the nociceptive ion channel, TRPA1

C. Doran and G. Reid

Department of Physiology, University College Cork, Cork, Ireland

Transient receptor potential A1 (TRPA1) is an ion channel receptor that specifically responds to noxious compounds such as cinnamaldehyde and bradykinin. TRPA1 is thought to be involved in various pain pathways, including cold allodynia and mechanical hyperalgesia. It is co-expressed with the capsaicin receptor, TRPV1, in primary sensory neurones. We have previously reported that activation of TRPV1 leads to a desensitisation of TRPA1, through a calcium-dependent mechanism. Here, we further the case for the involvement of elevated $[Ca^{2+}]_i$ in TRPA1 inhibition and uncover the role of other second messengers that act downstream of TRPV1 activation.

Adult Sprague-Dawley rats were killed by 100 % CO2 inhalation followed by decapitation, and dissociated DRG neurones cultured with nerve growth factor for 12-24 hours. Responses of individual neurones to all compounds were evaluated using Calcium Green-1 microfluorimetry ($\Delta F/F_0$).

Previously, we have shown that 1 μM capsaicin and 50mM KCL elicit comparable rises in $[Ca^{2+}]_i$ in TRPV1 positive neurones and that in both cases this leads to a desensitisation of TRPA1. We now further report that TRPA1 responsiveness to cinnamaldehyde (200 μM) remains intact following activation of TRPV1 by capsaicin (1 μM) in reduced $[Ca^{2+}]_i$ conditions. In nominally calcium-free extracellular solution, the response to cinnamaldehyde was reduced (by 30 %), but not abolished, by preceding application of capsaicin.

We conclude that calcium is a crucial second messenger involved in TRPV1-mediated inhibition of TRPA1. We propose that pharmacological targeting of second messengers could be a potential avenue for blunting TRPA1-mediated nociception.

We wish to thank the Health Research Board, Ireland for funding this work.

Where applicable, the authors confirm that the experiments described here conform with The Physiological Society ethical requirements.

PC38

The contribution of melanopsin-driven photoreception to light-evoked activity within the mouse olivary pretectal nucleus

A.E. Allen, T.M. Brown, J. Gigg and R.J. Lucas

Faculty of Life Sciences, University of Manchester, Manchester, UK

In addition to rod and cone photoreceptors, the retina contains a subset of retinal ganglion cells that are rendered intrinsically photosensitive due to the expression of the photopigment melanopsin. These cells, termed mRGCs (melanopsin-expressing retinal ganglion cells), innervate several central targets, notably those associated with non-image forming responses to light. One such area is the olivary pretectal nucleus (OPN), a relay-station for the pupillary light reflex.

We aimed to characterise the contribution of melanopsin-photoreception to light-evoked activity within the OPN *in vivo*. To achieve this, changes in spike-firing rate were assessed via multi-electrode recordings in the pretectum of mice anaesthetised with urethane (1.5g/kg). Responses to increasing intensities of blue (460nm) and red (640nm) light were measured, for both short (2s) and long (30s) duration stimuli. To isolate rod/cone vs. mRGC-driven activity, we compared responses in wildtype mice with those of *rodless+coneless* mice, and melanopsin knockout (*Opn4*$^{-/-}$) mice.

Light responses within the wildtype OPN were characterised by strong transient increases in firing rate at lights ON and OFF, and sustained elevations in firing rate for the duration of stimulus presentation. Responses showed irradiance-dependent increases in amplitude and response speed at intensities ranging from 9.8 to 15.8 $\log_{10}$ photons/cm^2/sec. In *rodless+coneless* mice, transient increases in firing rate were entirely absent. Instead, neurons typically showed sluggish increases in firing rate that gradually increased to a peak around 10s after stimulus onset, and persisted for around 20s after offset. The *rodless+coneless* OPN also was much less sensitive, with a threshold for detectable responses around 13.8 $\log_{10}$ photons/cm^2/sec. Conversely, *Opn4*$^{-/-}$ mice retained fast ON and OFF transient responses as seen in wildtypes, but showed relatively little sustained responses throughout light stimuli. The sensitivity of *Opn4*$^{-/-}$ mice was similar to that of wildtype mice, with irradiance-dependent responses occurring in the range of 9.8 to 15.8 $\log_{10}$ photons/cm^2/sec.

These data reveal that while rod and cone photoreceptors drive the fast transient responses to light onset and offset, melanopsin contributes to sustained elements of light-evoked activity within the OPN, especially at higher light intensities. They further suggest that melanopsin makes a unique contribution to the sensory capabilities of the mammalian visual system.

This work was supported by the BBSRC and the University of Manchester Alumni Fund.

Where applicable, the authors confirm that the experiments described here conform with The Physiological Society ethical requirements.

PC39

Thalamic extrasynaptic GABAA receptors are required for typical absence seizures

G. Di Giovanni, G. Orban, S.J. Fyson, V. Crunelli and D.W. Cope

School of Bioscience, Cardiff University, Cardiff, UK

Aberrant GABAergic inhibition in thalamo-cortical networks has been identified as a potential mechanism for spike-and-wave discharge (SWD) generation. Thalamocortical (TC) neurons in the ventrobasal (VB) thalamus receive both 'phasic' and 'tonic' GABAA receptor mediated inhibition, generated by synaptic and extrasynaptic delta-subunit containing receptors, respectively [Cope et al., 2005; J. Neurosci. 25: 11553]. We have shown a selective increase of tonic GABAA receptor-mediated inhibition in pharmacological as well as in polygenic and monogenic rat and mouse models of absence epilepsy due to an impairment of GABA transporter-1 (GAT-1) activity [Society for Neuroscience 2007, 142.7, 142.8, 142.9]. Therefore, we suggested that extrasynaptic GABAA receptor gain-of-function in VB TC neurons is a necessary requirement for the appearance of SWDs.

To directly test this hypothesis, we have now pharmacologically and genetically targeted extrasynaptic GABAA receptors in VB and monitored EEG and behavioural correlates of absence epilepsy in normal Wistar rats, Genetic Absence Epilepsy Rats from Strasbourg (GAERS) and GABAA receptor delta-subunit knockout mice. All experiments were conducted in accordance with the UK Animal Scientific Procedure Act. Reverse microdialysis of the selective extrasynaptic GABAA agonist THIP (70 and 100 μM, both n=5) and the selective GAT-1 inhibitor NO-711 (200 μM, n=5) into the VB induced SWDs and behavioural correlates of absence seizures in normal Wistar rats. THIP- and NO-711-induced SWDs were suppressed by systemic administration of the anti-absence drug ethosuximide (ETX, 100 mg/kg, n=5). In addition, we "knocked-down" extrasynaptic GABAA receptors in TC cells of GAERS by directly infusing a δ subunit specific antisense oligodeoxynucleotide (ODN, 1 and 2 nMol/μl, n=5 and 6, respectively) into the VB. The antisense ODN produced a marked reduction (~70% at 2 nMol) of the total time spent

in seizures and the number of SWDs, whilst infusion of a missense ODN (1-2 nMol/μl, n=5) was ineffective. Lastly, systemic administration of 50 mg/kg of gamma-butyrolactone induced absence seizures in wild type mice, which were significantly reduced in the delta-subunit knockout mice (84% decrease in the total time spent in seizures and 53% reduction in number of SWDs).
Our data demonstrate that extrasynaptic GABAA receptor gain-of-function in VB TC neurons is a necessary and sufficient requirement for the appearance of a pure absence epilepsy phenotype, and that GAT-1 critically controls SWD genesis.

This work was supported by the Wellcome Trust. D.W. Cope is an Epilepsy Research UK Fellow.

Where applicable, the authors confirm that the experiments described here conform with The Physiological Society ethical requirements.

PC40

Effects of TTA-P2, a novel potent and selective T-type calcium channel blocker on thalamic cell excitability

N. Leresche[2], F.M. Dreyfus[2], A. Tscherter[2], A.C. Errington[1], V. Crunelli[1] and R.C. Lambert[2]

[1]School of Bioscience, Cardiff University, Cardiff, UK and [2]UMR7102 UPMC-CNRS, Paris 75005, France

Although it is well established that low-voltage activated T-type Ca2+ channels play a key role in many neurophysiological functions and pathological states, the lack of selective and potent antagonists has so far hampered a detailed analysis of the full impact that these channels might have on single cell and neuronal network excitability as well as on calcium homeostasis.
Using thalamic slices (prepared from fully anaesthetized Wistar rats or transgenic mice, in accordance with the UK Scietific Procedure Act), we now show that the novel piperidine-based molecule TTA-P2 exerts a specific, potent (IC50: 22nM) and reversible inhibition of T-type Ca2+ currents (IT) in both thalamocortical (TC) and reticular thalamic nucleus (NRT) neurons without any action on HVA Ca2+ currents. Under current clamp conditions, 1μM TTA-P2, a concentration that fully blocks IT (96±1%, n=7), has no effect on tonic firing and action potential characteristics (threshold, half-width, amplitude, afterhyperpolarization), but abolishes the low threshold Ca2+ potential (LTCP)-dependent high frequency burst firing of thalamic neurons. In addition, when TC and NRT neurons are held at -60mV, application of 1μM TTA-P2 produces a tonic hyperpolarization of 3.1±0.5mV (n=11) and 5±2.2mV (n=6), respectively. Such hyperpolarization is not observed when TC neurons are held at -70mV or in TC neurons from Cav3.1 KO mice that are recorded at -60mV (n=6). These data demonstrate that the TTA-P2 induced hyperpolarization is due to the block of the window component of IT and that this current contributes to the resting membrane potential of thalamic neurons. In addition, we could show that application of 1μM TTA-P2 blocks membrane potential bistability of TC neurons in slices that are perfused with the h-channel blocker ZD 7288 (100μM) (n=4). Thus, the use of TTA-P2 has allowed to consolidate and enlarge our current understanding of the contribution of IT to single TC neuron excitability, and to provide the first direct demonstration that the window component of IT underlies the intrinsically generated slow (<1Hz) sleep oscillation of thalamic neurons.

Where applicable, the authors confirm that the experiments described here conform with The Physiological Society ethical requirements.

PC41

Integrative *in vivo* approaches to studying anaesthetic mechanisms

D.R. Carr

Department of Biophysics, Imperial College, London, UK

Although modern general anaesthesia has been used for over 100 years in medical and veterinary practice, the mechanisms of how such a wide variety of pharmacological agents induce reversible loss of consciousness are not completely known (Franks, 2008). Given that loss of consciousness can only be measured in live animals, in vivo experiments therefore provide the most optimal setting for the elucidation of such unknowns.
Electroencephalographic (EEG) methods have been widely used in both research and clinical settings to monitor anaesthetic depth for surgical and non-surgical procedures in humans and animals. The technique relies on recording network activity of synchronously oscillating neurons in the mammalian brain. The utility of the technique is that it can provide a real-time measure of brain activity on millisecond timescales.
We recorded the EEG activity of C57BL/6 mice chronically implanted (under ketamine (80 mg/kg) and xylazine (15 mg/kg) mix anaesthesia) with gold-plated electrodes in response to increasing doses of the volatile anaesthetic halothane. We recapitulated experiments that show a prominent theta oscillation (centred at 5 Hz) in the EEG and found this effect to be sensitive to muscarinic antagonism with atropine (50 mg/kg i.p. or 50 μg bolus in the medial septum) (Pang et al., 2009).
There is evidence that this theta oscillation results from the concerted action of cholinergic and GABAergic neurotransmitter systems in the medial septum that form projections to the hippocampus (Yoder & Pang, 2005). So for our further investigations we injected various pharmacological agents directly into the medial septum thus allowing a more specific neurophysiological analysis.

Franks, NP (2008) Nat Rev Neurosci 9(5): 370-86.

Pang, DS et al. (2009) Proc Natl Acad Sci, 106, 17546-51.

Yoder, RM & Pang, KC (2005) Hippocampus 15(3): 381-92.

Funded by BBSRC and CIMPP.

Where applicable, the authors confirm that the experiments described here conform with The Physiological Society ethical requirements.

PC42

Anatomical and physiological aspects of the rat cerebellar olivo-cortico-nuclear system

N. Cerminara[1], I. Sugihara[2] and A. Richard[1]

[1]Department of Physiology & Pharmacology, University of Bristol, Bristol, UK and [2]Systems Neurophysiology, Tokyo Medical and Dental University, Tokyo, Japan

The main information processing part of the cerebellum is its cortex, and its sole output is via the Purkinje cells which directly inhibit the neurones of the cerebellar nuclei. The cortico-nuclear pathway is thus central to cerebellar operations. An important organizational principle of the cerebellum is a division into a series of rostrocaudally-oriented olivo-cortico-nuclear modules. Some correspondence between the spatial location of these cortical component of these modules (zones) and the distribution of Purkinje cells that express zebrin II has also been found. Detailed electrophysiological mapping studies suggest that the cortical zones can be split into smaller units.
The aim of the present investigation is two-fold:
1. To study the topographical organization of the interpositus nucleus in relation to its anatomical connectivity, zebrin II immunocytochemistry and physiological responses at this subzonal level of organization.
2. To examine the relationship between Purkinje cell and corticonuclear activity within the same module target.
In barbiturate (60 mg/kg i.p) or urethane (1.3 g/kg i.p) anaesthetized adult Wistar rats we used percutaneous electrical stimulation of the ipsilateral forelimb, tail and different parts of the ipsilateral hindpaw to evoke climbing fibre field potentials in the C1 zone in the paramedian lobule and copular pyramidis. In anatomical studies, the evoked responses were used to guide nanoinjections of bidirectional tracer (fluorescent beads and BDA) into the cortex and after a survival period of 7 days the animals were deeply anaesthetised and the brains were removed for histological analysis. Injection sites were mapped relative to zebrin II stripes; beads-labelled olive cells were mapped onto transverse and horizontal maps of the inferior olive; and BDA-labelled Purkinje cell terminals were mapped onto a 3D template of the cerebellar nuclei. In physiological studies, simultaneous cerebellar cortical and nucleus interpositus anterior recordings were carried out in response to electrical stimulation of the forelimb and hindlimb in areas known to receive cortico-nuclear projections from the C1 zone.
Preliminary anatomical results suggest that a detailed subzonal topography is present within the C1 zone in which climbing fibre responses, zebrin stripes and olivo-cortico-nuclear connections are correlated. Our physiological data demonstrates that evoked positive field potentials in the nucleus interpositus anterior and climbing fibre potentials in the cerebellar cortex are positively correlated. Preliminary experiments of single unit recordings suggest a complex pattern of interactions between Purkinje cells and cerebellar nuclear cells within the same module.

This work is supported by the Wellcome Trust and a Benjamin Meaker Visiting Professorship

Where applicable, the authors confirm that the experiments described here conform with The Physiological Society ethical requirements.

PC43

Substance MCS-18 from Helleborus purpurascens inhibits capsaicin and acid induced activation of TRPV1

C. Neacsu[1], A.C. Ciobanu[1], O. Toader[1], G. Szegli[2], F. Kerek[3] and A. Babes[1]

[1]Department of Animal Physiology and Biophysics, University of Bucharest, Bucharest, Romania, [2]Cantacuzino Institute for Microbiology and Immunology, Bucharest, Bucharest, Romania and [3]Donatur GmbH, Martinsried, Germany

Extracts from the roots of the plant Helleborus purpurascens have been traditionally used in Balkan folk medicine for their anti-nociceptive activities. The aim of this work was to asses the effects of substance MCS-18, extracted and purified from Helleborus roots, on TRPV1 a well known polymodal receptor involved in nociception, in rat DRG neurons. DRG neurons were held in primary culture for 24 hours. TRPV1 was also expressed and tested in HEK293 cells. Neurons and HEK293 cells were analyzed with microfluorimetry, using the calcium indicator Calcium Green-1 AM and the patch-clamp technique. MCS-18 inhibited responses to capsaicin 300 nM when the agonist was applied five times, repeatedly (DF/F0 was 0.03 for the third response [MCS-18 was co-applied] compared to 0.21 for the 2nd response, n = 25; $p < 0.0001$). When MCS-18 was pre-applied it decreased the capsaicin responses from 0.55 ± 0.05 to 0.43 ± 0.06 ($p < 0.05$). Activation by acid pH (5.5) in DRG neurons, was also reduced by about 44% (0.14 ± 0.03 compared to 0.25 ± 0.02, n = 32, $p < 0.01$). Inhibition of pH responses was mediated by TRPV1, because MCS-18 had no effect on ASIC channels. Also, the substance had no effect on the increases in [Ca2+]i evoked by the TRPA1 agonist cinnamaldehyde. MCS-18 did not inhibit heat (45 oC) responses. Inhibition of capsaicin (2 μM) activation was dose-dependent as confirmed by whole-cell patch-clamp (from 5% inhibition at 0.01 μg/ml, to 90% inhibition at 10 μg/ml). Moreover capsaicin currents were also inhibited in excised outside-out patches in DRG neurons. When expressed in HEK293 cells, rTRPV1 responses to capsaicin are inhibited by MCS-18, and the magnitude of the inhibition was 84% as shown by calcium imaging experiments. The same effect was shown by patch-clamp data. The antagonistic effect of MCS-18 on TRPV1 activation by capsaicin and protons may be important in pain therapy.

Where applicable, the authors confirm that the experiments described here conform with The Physiological Society ethical requirements.

PC44

State-dependent spatio-temporal calcium dynamics in dendrites of thalamocortical neurons

A.C. Errington and V. Crunelli

School of Bioscience, Cardiff University, Cardiff, UK

During wakefulness thalamocortical (TC) neurons are typically depolarised and fire 'tonic' Na2+-mediated action potentials (APs), whereas during sleep they are more hyperpolarised and

typically fire 'bursts' of APs that are driven by low threshold Ca2+ spikes (LTS). In many other neurons, including pyramidal neurons, APs have been demonstrated to actively backpropagate far into the dendritic tree and play a major role in synaptic integration. Using patch clamp recording and two photon Ca2+ imaging (Fluo 5F/Fluo 4FF and Alexa 594, G/R), we studied dendritic Ca2+ changes evoked by tonic APs and LTS-mediated AP bursts in TC neurons of the lateral geniculate nucleus. Thalamic slices were prepared from Wistar rats that had been fully anaesthetized with isoflurane in accordance with the UK Animal Scientific Procedure Act. LTS evoked by somatic current injection (50 ms, 50-180 pA) into TC neurons held at -72.4 ± 0.3 mV produced quasi-synchronous global dendritic Ca2+ transients that were temporally aligned with the somatic voltage inflection, which signifies the onset of the LTS, and that were significantly larger in distal dendrites (< 50 μm, $\Delta G/R = 0.17 \pm 0.02$; >100 μm, 0.26 ± 0.02, n = 8, $P < 0.05$, one-way ANOVA). LTS evoked Ca2+ transients were also significantly larger than bursts of 3 bAPs evoked at 200 Hz (3bAPs, $\Delta G/R = 0.06 \pm 0.007$, $P < 0.05$) and reduced significantly by TTX (500 nM, $P < 0.05$, n = 6). In marked contrast, trains of APs (10-50 Hz, 500 ms) evoked somatically (2 ms, 1-1.5 nA) from a holding potential of -50 mV produced Ca2+ elevations that were spatially restricted to proximal dendrites (30 Hz, < 50 μm, 0.129 ± 0.011; >100 μm, 0.006 ± 0.001, n = 8, $P < 0.001$). In proximal dendrites Ca2+ increases were linearly related to tonic firing frequency (10 Hz, 0.037 ± 0.004; 30 Hz, 0.095 ± 0.014; 50 Hz, 0.17 ± 0.019, n = 7) and plateau levels matched predictions based upon single bAP evoked transients. Moreover, τdecay for each train was not significantly different from τdecaybAP indicating that Ca2+ extrusion is also linearly related to activity during tonic firing at frequencies up to 50 Hz. Unlike LTS Ca2+ transients bAP transients were completely abolished in TTX. LTS evoked Ca2+ transients in distal dendrites were significantly reduced by focal 'puffed' applications of the T-type calcium channel antagonist TTA-P2 but were not significantly reduced in TTX.
These results demonstrate, for the first time, the presence of T-type calcium channels in distal dendrites of TC neurons and highlight the spatial and temporal differences in dendritic calcium signalling during the classical 'tonic' and 'burst' firing modes.

This work was supported by the Wellcome Trust.

Where applicable, the authors confirm that the experiments described here conform with The Physiological Society ethical requirements.